UNIVERSITA' DELLA CALABRIA

Dipartimento di Farmacia e Scienze della Salute e della Nutrizione

Dottorato di Ricerca in Medicina Traslazionale

(XXXVI ciclo)

"The Receptor for Advanced Glycation End Products (RAGE) prompts the motility of breast cancer cells through EphA3"

Settore Scientifico Disciplinare: **SSD MED/04**

Supervisore

Prof.ssa Rosamaria Lappano

Dottoranda

Dott.ssa Asia Spinelli

Coordinatore del Dottorato

Prof.ssa Stefania Catalano

ANNO ACCADEMICO 2022/2023

Alle donne: fate casino.

INDEX

ABSTRACT

The receptor for advanced glycation-end products (RAGE) and its ligands have been associated with obesity, inflammation and diabetes. Recently, several studies showed that RAGE signaling may contribute to the metastatic progression of breast cancer (BC), although the mechanisms underlined remain to be fully characterized. Here, we aimed at defining the molecular events by which RAGE may prompt aggressive features in estrogen receptor (ER)-positive BC cells. As model system, we engineered human MCF7 and T47D BC cells to stably overexpress RAGE. The RAGE-mediated changes in cell morphology, migration, invasion and colony formation were evaluated *in vitro* through scanning electron microscopy, migration, invasion and clonogenic assays, while *in vivo* effects were explored in zebrafish xenografts models. Importantly, high-throughput RNA sequencing allowed us to analyze the transcriptomic landscape of RAGE-overexpressing BC cells. Thereafter, Gene Ontology (GO) and Kyoto Encyclopedia of Genes and Genomes (KEGG) pathway enrichment analyses were performed to recognize the biological functions of the differentially expressed genes (DEGs) identified in RAGE-overexpressing respect to wild type BC cells. Molecular biology techniques, including flow cytometry, real-time PCR, chromatin immunoprecipitation, immunofluorescence and Western blot assays, were employed to investigate the molecular mechanisms implicated in the regulation of a novel RAGE target gene named EphA3. The clinical significance of EphA3 was explored in the TCGA cohort of BC patients through the survivALL package, whereas the involvement of EphA3 in mediating migratory and invasive effects was ascertained in both BC cells and important component of the tumor microenvironment like cancer-associated fibroblasts (CAFs). Our findings revealed that RAGE-overexpressing BC cells exhibit an enhanced dissemination potential respect to wild type BC cells. Moreover, we have found that EphA3 may act as a main mediator of the RAGE-induced motility of BC cells and CAFs. Overall, our findings suggest that EphA3 may be considered as a novel RAGE target gene that may prompt BC cell migration and invasion. Therefore, these data highlight the potential significance of targeting

RAGE and EphA3 in the treatment of BC, particularly in diabetic or obese patients that show high RAGE levels.

1. INTRODUCTION

1.1 Breast Tumor

Breast cancer (BC) is the most common malignancy and the second leading cause of cancer related death in women worldwide. Although localized disease is largely curable, metastatic or recurrent disease carries an unfavorable prognosis (1). The management of BC has changed considerably in the last two decades with significant improvements in systemic therapy and advances in surgical techniques (2). As a result of the early detection and more efficient therapeutic options, BC mortality is decreasing in developed countries (3).

There are two major categories of BC:

- Non-invasive BC: carcinoma (in situ) characterized by non-invasive malignant epithelial cells that cannot pass the basal membrane, thus not reaching lymph nodes. This cell can be located at lobular level (*lobular carcinoma in situ*: it is a sign of increased risk of forming tumors in both breasts) or can involve the duct of the gland (*ductal carcinoma in situ*: it is an initial form of BC limited to cells that form the wall of the ducts. If it is not identified promptly, it can become invasive). This type of BC can be additionally subdivided into intraepithelial ductal neoplasia (DIN) (carcinoma in situ) and lobular intraepithelial neoplasia (LIN).
- Invasive BC: infiltrating carcinoma characterized by the crossing of the basal membrane and the presence of stromal invasion and diffusion at the lymphatic level. It is possible to distinguish *infiltrating ductal carcinoma* (it passes the duct wall and represents the largest percentage of all forms of BC) and *infiltrating lobular carcinoma* (the tumor surpasses the lobule wall; it can simultaneously attack both breasts or appear in multiple spots in the same breast).

Many risk factors lead to breast malignancy development:

- Age and gender. The risk of developing BC increases with age. Most advanced BC cases are found in women over age 50 (4). Women are 100 times more likely to get BC than men are.
- Family history of BC. You may also have a higher risk for BC if you have a close relative who has had breast, uterine, ovarian, or colon cancer. About 20-30% of women with BC have a family history of the disease.
- Genes. Some people have genes that make them more likely to develop BC. The most common gene defects are found in the BRCA1 and BRCA2 genes. These genes normally produce proteins that protect you from cancer. If a parent passes you a defective gene, you have an increased risk for BC. Women with one of these defects have up to an 80% chance of getting BC sometime during their life (5).
- Menstrual cycle. Women who got their periods early (before age 12) or went through menopause late (after age 55) have an increased risk for BC (6).

Other risk factors include:

- Dietary and metabolic factors: it has been demonstrated that a high-lipid diet can promote the development of different spontaneous, transplanted or chemically induced neoplasms in laboratory animals (7-10)
- Smoking: it represents a risk factor for the majority of malignancies, including BC (11-13).
- Radiation. The radiation therapy to treat cancer of the chest area, increase higher risk to develop BC (14).

BC can be diagnosed with mammography and breast ultrasound, while in specific circumstances magnetic resonance imaging may be a further option (15). Treatment is based on many factors, including type, stage and molecular subtypes of the cancer. In general, cancer treatments may include chemotherapy medicines to kill cancer cells, radiation therapy to destroy cancerous tissue, surgery to remove neoplastic tissue, lumpectomy removes the breast lump, mastectomy removes all or part of

the breast and hormonal therapy. Chemotherapy is helpful, but not always necessary and it has to be prescribed after a personalized evaluation. It is also prescribed for the initial forms for precautionary purposes and the benefit, in terms of years of survival, is greater than the most advanced tumor forms. In the last few years, it became diffused the use of neoadjuvant chemotherapy, administered before the surgery to reduce the dimension and the aggressiveness of the tumor (16).

Breast tumors are classified in five stages:

- Stage 0: also called carcinoma in situ comprising lobular carcinoma in situ and ductal carcinoma in situ.
- Stage I: it is a tumor at the initial phase; it has a diameter less than 2 cm and it do not involve lymph nodes.
- Stage II: it is a tumor at the initial phase with less than 2 cm of diameter, but it already reached axillary lymph nodes; it could also be a tumor bigger than 2 cm without the implication of lymph nodes.
- Stage III: it is a locally advanced tumor of variable dimensions that already got to the axillary lymph nodes or that involves the tissues near the breast (for example the skin).
- Stage IV: Is a metastatic cancer that has involved other organs outside the breast.

However, more extensive studies derived from cDNA microarrays and based on gene variations have made possible further classification of BCs into five intrinsic subtypes: luminal A, luminal B, human epidermal growth factor receptor 2 (HER2)-enriched, basal and normal-like (17).

- Luminal A BC is positive for estrogen receptors (ER) and progesterone receptors (PR), negative for HER2, and show low levels of the Ki-67 protein, which plays a role in regulating cancer cell growth. Luminal A tumors typically exhibit a slower growth rate compared to other types of BC, a lower grade and generally have a favorable prognosis.
- Luminal B subtypes express ER, but it is negative for HER2. Additionally, it exhibits either elevated levels of Ki-67, signifying accelerated cancer cell growth, or it is PR-negative.

- HER2-enriched BC lacks ER and PR but is positive for HER2. Typically, HER2-enriched tumors exhibit a faster growth rate compared to luminal cancers and may have a less favorable prognosis. However, they are often effectively treated with targeted therapy medications designed to address the HER2 protein.
- Triple-negative or basal-like BC is ER, PR and HER2-negative and is considered the more aggressive BC subtype.

Based on these considerations, the analysis of prognosis and therapeutic treatment is defined on the immunohistochemical evaluation of the endocrine receptors for estrogen and progesterone (ER and PR, respectively), and HER2. Breast tumors that lack expression of the above indicated receptors are defined triple negative BC (TNBC) and are characterized by high rates of tumor recurrence and poor overall compared to those with other BC subtypes (18).

1.2 The tumor microenvironment

The cancer microenvironment is a key contributor of malignant progression (19). It consists of cellular components surrounding cancer cells, like fibroblasts, macrophages, immune cells, adipocytes and endothelial cells as well as non-cellular components like the extracellular matrix (ECM) (Fig.1.2.1).

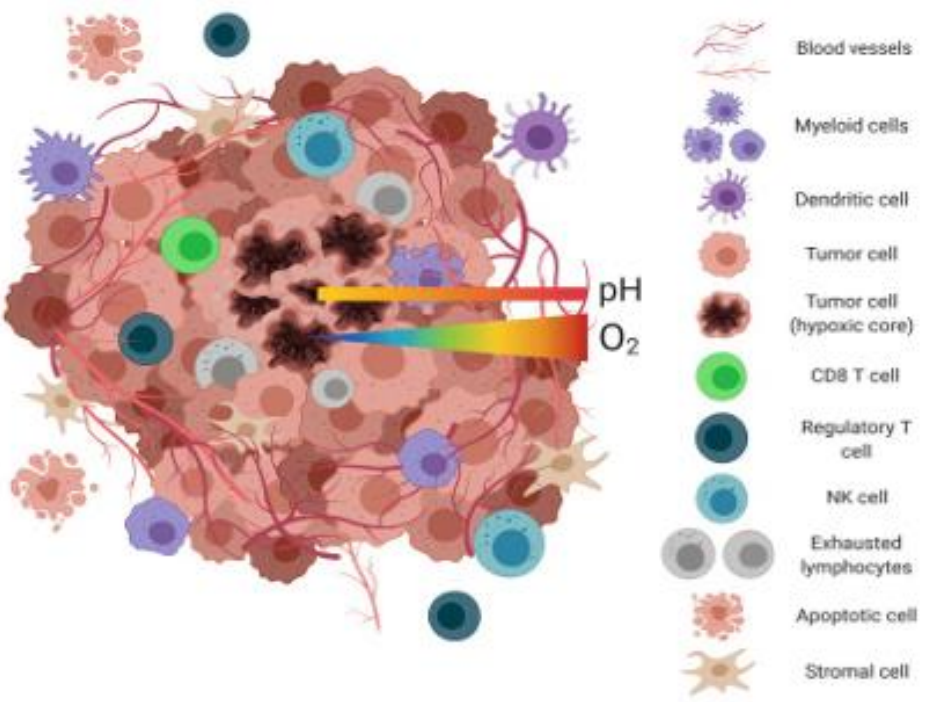

Fig. 1.2.1 Tumor Microenvironment

Over the last years, multiple evidence has highlighted the importance of the crosstalk between tumor cells and the surrounding stroma. Stromal cells may influence the behavior of epithelial cells by secreting a range of ECM proteins, chemokines, cytokines and growth factors (20). Among the main components of the tumor microenvironment, cancer-associated fibroblasts (CAFs) are acknowledged stimulator of cancer progression toward an aggressive phenotype (21-22). Extensive evidence indicates that a high amount of CAFs within the tumor microenvironment correlates with poor clinical prognosis in diverse malignancies, including BC (23). CAFs are α-smooth muscle actin positive, spindle-shaped, blast-like cells. Differentiation of CAFs from other cell types, such as local fibroblasts, hepatic stellate cells, mesenchymal stem cells, endothelial and epithelial cells, is mainly mediated by transforming growth factor-β 1 (TGF-β 1), although other factors, such as growth factors, chemokines, epigenetic regulators and oxidative stress may also play a role in CAFs differentiation (24-26). Phenotypically, CAFs closely resemble normal myofibroblasts, but they express specific markers, such as fibroblast activation protein (FAP), fibroblast-specific protein 1,

neuronglial antigen-2, vimentin, Thy-1, tenascin (TN)-C, periostin (POSTN), palladin or podoplanin (PDPN) that differentiate them from normal fibroblasts and contribute to their enhanced proliferative and migratory capacities both *in vitro* and in *vivo* (27-28). Recent advances in immunotherapy demonstrate that targeting CAFs may represent a powerful tool in the management of tumor progression and to predict therapeutic responses (29). In this regard, several preclinical studies have been developed to prevent the pro-tumorigenic function exerted by CAFs, demonstrating excellent clinical results (30).

1.3 The receptor for advanced glycation end-products (RAGE)

The receptor for advanced glycation end-products (RAGE) is a member of the immunoglobulin protein family of cell surface molecules (31) and shares structural homology with other immunoglobulin-like receptors. In addition to advanced glycation end-products (AGEs), RAGE can bind to different ligands including high-mobility group protein (B)1 (HMGB1), S-100 calcium-binding protein, amyloid-β-protein, Mac-1 and phosphatidylserine (32). The gene encoding RAGE is located on chromosome 6 next to the MHC class III complex region and the homeobox gene HOX12 and the human counterpart of the mouse mammary tumor gene int-3 (33). The mature 382 amino-acid long RAGE is composed of an extracellular domain (85 aa), a single transmembrane spanning helix (27 aa) and a short cytosolic region (41 aa). The extracellular domain of RAGE contains one variable, like V-domain, and two constants, like C type domains, which are frequently referred to as C1 and C2 domains. Recent studies suggest that RAGE can form oligomers at the cell surface (33). RAGE and many of its ligands are overexpressed in diabetes, chronic inflammation, and various malignancies (34-35).

RAGE engagement activates multiple signaling pathways (Fig. 1.3.1) including reactive oxygen species, p21-ras, erk1/2 (p44/p42) mitogen-activated protein kinases, p38. RAGE possesses two N-glycosylation sites, one adjacent to the V-domain and the second one located within the V-domain SAPK/JNK mitogen-activated protein kinases, RhoGTPases, phosphoinositol-3 kinase and JAK/STAT pathway, with important downstream inflammatory consequences, such as the activation of nuclear factor-kappaB (NFκB), AP-1 and STATs, which are involved in the inflammatory process seen in both diabetes and cancer (34). Consequently, the RAGE-mediated activation of the aforementioned signaling pathways has been reported to stimulate oxidative stress and inflammation leading to the growth and metastasis of diverse types of tumors, including BC (34-38). In particular, the RAGE-induced activation of MAPK, PI3K/Akt, JAK/STAT and NF-κB transduction pathways triggers the production of pro-inflammatory cytokines and growth factors that in turn promote cancer cell survival, proliferation, migration, invasion and angiogenesis (39).

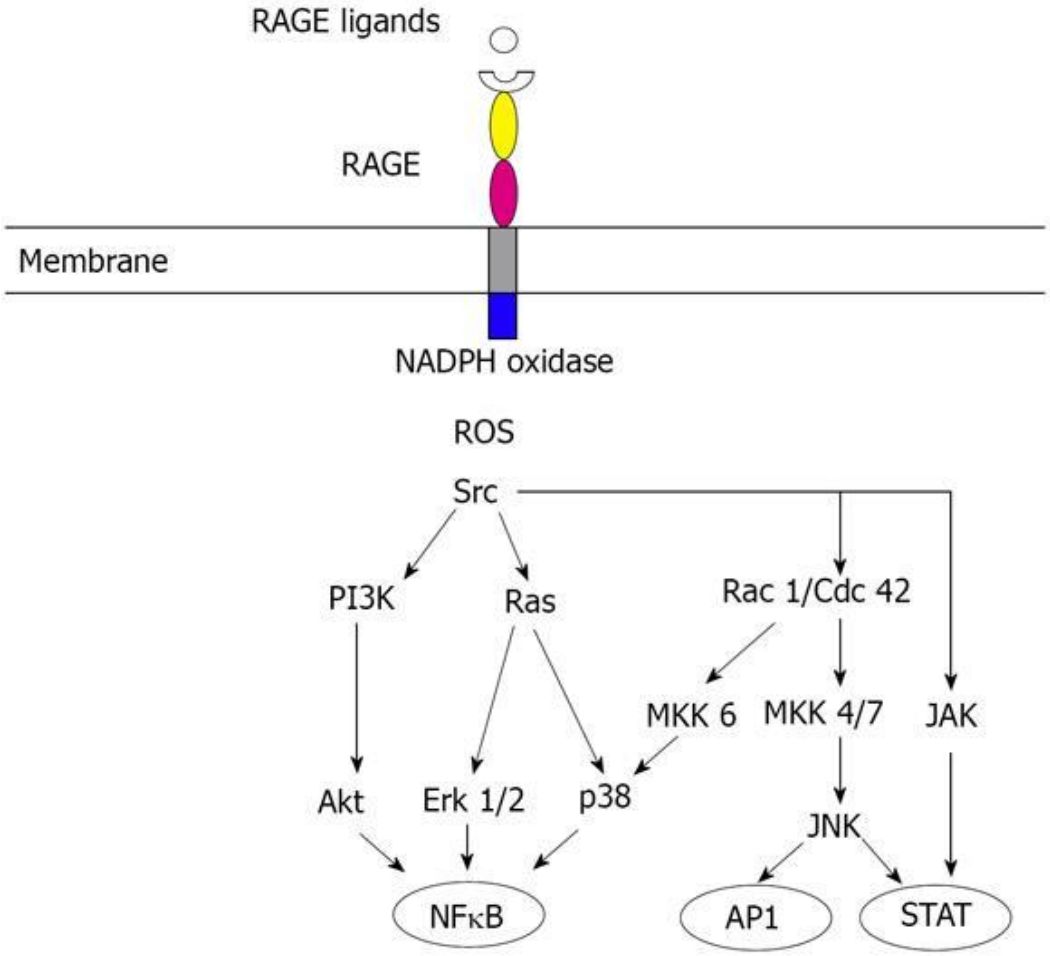

Fig. 1.3.1 RAGE Signaling Pathway

In accordance with these findings, it has been demonstrated that RAGE-mediated signaling plays a role in the crosstalk between malignant cells and the surrounding tumor microenvironment (TME). This crosstalk is crucial for sustaining various aspects of cancer, including growth, angiogenesis, autophagy and metastatic dissemination (37, 39).

1.4 The Eph-Ephrin system

Eph receptors represent the largest subfamily of receptor tyrosine kinases (RTKs). Along with Eph ligands namely ephrins, Eph are important mediators of cell–cell communication regulating cell attachment, shape and mobility (40). Like all RTKs, Eph are transmembrane proteins and their structure features an N-terminal domain required for the interaction with ligands and a cytoplasmic region containing a juxtamembrane segment, followed by a highly conserved kinase domain which catalyzes tyrosine phosphorylation of protein substrates (41). Eph receptors and their cognate ligands are both divided into two subclasses, A and B, based on the sequence conservation and their binding affinities. In general, the eight different EphA RTKs (EphA1–A8) promiscuously interact with five A-ephrins (ephrinA1–A5), which are attached to the cell via a glycosylphosphatidylinositol (GPI) linkage. The EphB subclass receptors (EphB1–B6) interact with three different B-ephrins (ephrinB1–B3), which are attached to the cell through a hydrophobic transmembrane region and a short cytoplasmic domain (42). A singular feature of ephrins and Eph receptors is their ability to induce a bi-directional signaling (FIG 1.4.1). An Eph receptor can act as a ligand in the same way that an ephrin ligand can act as a receptor.

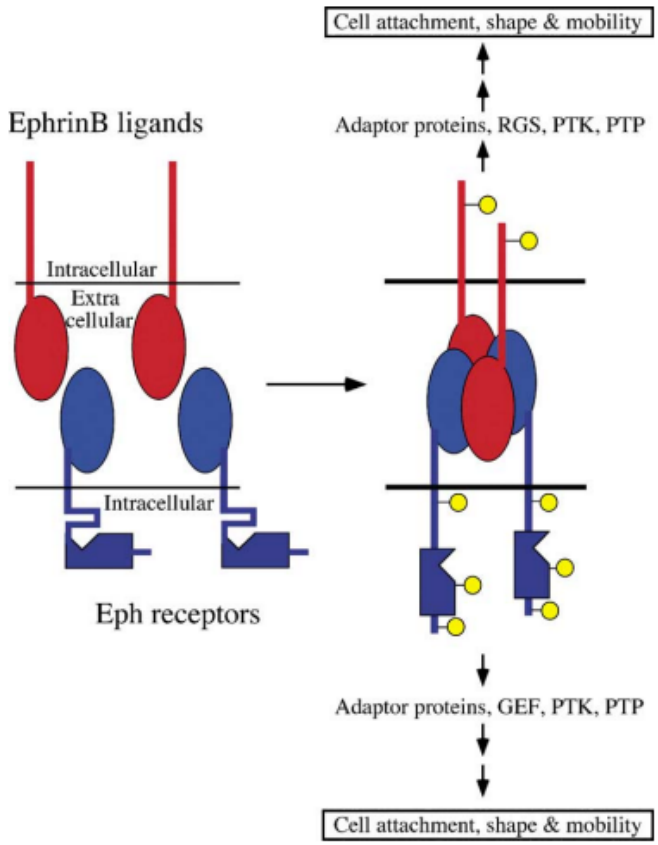

Fig. 1.4.1 Activation of the Eph–ephrin bi-directional signaling pathway.

Upon cell–cell contact, both Eph receptors and ephrins can activate signal transduction pathways within either the cells expressing the ligand or those presenting the receptor. The signaling initiated by Eph receptors bound to ephrin is termed "forward signaling" and rely on the tyrosine kinase activity of the protein, while the signaling initiated by ephrins bound to Eph receptors is referred to as "reverse signaling" (43). The cellular responses to Eph receptor stimulation by their ephrin ligands are important in mediating a wide range of biological activities, including angiogenesis, cell segregation, attachment, shape and motility (44). Recently, many ephrins and Eph receptors have been shown to be up-regulated in tumors, especially in the more aggressive stages of tumor progression. Furthermore, an aberrant Eph expression has been reported to potentially increase the

metastatic potential. For instance, EphA2 mRNA overexpression has been detected in melanoma metastatic cell lines respect to primary tumors, while normal melanocytes do not show any expression (44). Similarly, EphB4 is overexpressed in several human BC cell lines and in primary, high grade, infiltrating, ductal breast carcinomas (45). In according to these data, several studies demonstrating the potential involvement of the Eph-Ephrin axis in the interactions between tumor cells and the associated tumor microenvironment. In particular, it has been reported that the Eph-Ephrin signaling can inhibit the movement of cancer cells through repulsive interactions and promote the migration of metastatic tumor cells toward the functional interplay with fibroblasts (46).

1.5 Aim of Study

The aim of the present study was to ascertain the potential involvement of RAGE in BC progression. In particular, we aimed to uncover novel transcriptional and molecular mechanisms whereby RAGE overexpression, which frequently occurs in diabetic and obese individuals, might contribute to migratory and invasive features in ER-positive BC. Furthermore, the transduction routes engaged by RAGE in triggering the cooperation between tumor and stromal cells toward BC progression have been explored.

2. Materials and Methods

2.1 Cell lines and establishment of RAGE-overexpressing stable clones. MCF7 and T47D BC cells were obtained from ATCC (Manassas, VA, USA), used less than 6 months after resuscitation, routinely tested and authenticated according to the ATCC suggestions. MCF7 cells were maintained in DMEM/F-12 with phenol red, supplemented with 10% fetal bovine serum (FBS) and 100 μg/ml penicillin/ streptomycin. T47D cells were maintained in RPMI 1640 with phenol red supplemented with 10% FBS, 0.2 Units/ml bovine insulin and 100 μg/ml penicillin/streptomycin. For stable transfection, MCF7 and T47D cells were seeded at 2×10^6 cells/well in a six-well plate and transfected with a pcDNA3-RAGE plasmid (a gift from Henri Huttunen, Addgene plasmid # 71435; http://n2t.net/addgene:71435; RRID:Addgene 71435) (47) or empty vector pcDNA3 using TurboFect™ Transfection Reagent (Thermo Fisher Scientific, Life Technologies Italia, Monza, Italy) according to the manufacturer's instructions. Stable clones were selected by continuously screening the above transfected cells with 500 μg/ml neomycin G418 (Merck Life Science, Milano, Italy). Afterwards, clones were maintained in the presence of 50 ng/ml neomycin to avoid loss of plasmids. RAGE overexpression in MCF7 and T47D cells was ascertained by immunoblotting experiments. All cell lines were grown in a 37 °C incubator with 5% CO_2.

2.2 CAFs. CAFs were isolated, cultured and characterized as previously described (48) from 10 invasive mammary ductal carcinomas and pooled for the subsequent studies. Briefly, specimens were cut into 1–2 mm diameter pieces, placed in a digestion solution (400 IU collagenase, 100 IU hyaluronidase, 10% FBS, antibiotics and antimycotics) (Thermo Fisher Scientific) and incubated overnight at 37 °C. After centrifugation at 90×g for 2 min, the super-natant containing fibroblasts was centrifuged at 485×g for 8 min; the pellet obtained was suspended in Medium 199 and Ham's F12 mixed 1:1 (supplemented with 10% FBS and 100 μg/ml penicillin/streptomycin). CAFs were then expanded into 10-cm Petri dishes and stored as cells passaged for three population doublings within a total 7 to 10 days after tissue dissociation. Primary cell cultures of fibroblasts were characterized by

immunofluorescence with human anti-vimentin (V9) and human anti-cytokeratin 14 (LL001) (Santa Cruz Biotechnology, DBA, Milan, Italy). FAPα antibody (H-56; Santa Cruz Biotechnology) was used to assess fibroblast activation (data not shown). We used CAFs passaged for up to 10 population doublings for the experiments to minimize clonal selection and culture stress, which could occur during extended tissue culture. CAFs were grown in a 37◦C incubator with 5% CO2 and switched to a medium without serum and phenol red the day before treatments to be processed for experiments.

2.3 Reagents. The EphA3 inhibitor AWL-II-38.3 was obtained from MedChem Express (DBA), mithramycin A (MMA) from Abcam (Euroclone S.p.A., Milan, Italy), CellTracker™ CM-DiI Dye from Thermo Fisher Scientific. All compounds were dissolved in dimethyl sulfoxide (DMSO).

2.4 RNA-Seq Pipeline. Total RNA from MCF7/wt and MCF7/RAGE cells was extracted using RNeasy mini kit according to manufacturer's instructions (Qiagen, Bioset s.r.l., Catanzaro, Italy). RNA integrity for library preparation was determined by analysis of extracted total RNA using a 2100 Bioanalyzer (Agilent Technologies) with RNA 6000 NanoChip. RNA concentrations were measured using Qubit RNA Assay Kit. Libraries were prepared from total RNA according to manufacturer instructions with Illumina Stranded mRNA Prep kit. Libraries quality was evaluated by size analysis on 2100 Bioanlyzer (Chip DNA HS) and concentrations were determined using Qubit DNA HS assay kit (Thermo Fisher Scientific). Sequencing was performed on Illumina Novaseq 6000 in the 100PE format. Reads preprocessing was performed by using fastp v0.20.0 (49), applying specific parameters in order to remove residual adapter sequences and to keep only high-quality data (qualified_quality_phred=20, unqualified_percent_limit=30, average_qual=25, low_complexity_filter=True, complexity_threshold=30). The percentage of uniquely mapped reads resulted high with the mean value of 84% (mean value for sample: 60 million total reads, unmapped reads 7%, quality base >q30 94%). Then, passing filter reads were mapped to the human genome reference (version GRCh38) using STAR v2.7.0 (50) with standard parameters, except for sjdbOverhang option set on read length. Genome and transcripts annotation provided as input were

downloaded from v99 of Ensembl repository. Alignments were then elaborated by RSEM v1.3.3 (51), to estimate transcript abundances. Subsequently, the sample-specific gene-level abundances were merged into a single raw expression matrix applying a dedicated RSEM command (rsem-generate-data-matrix). Genes with at least 10 counts in 50% of samples were then selected. Differential expression (pairwise comparisons) was computed by edgeR (52) from raw counts in each comparison. Re-annotation of previously differentially expressed genes (DEGs) was performed using the bioMart package (53) into R 3.6, querying available Ensembl Gene IDs and retrieving Gene Names and Entrez gene IDs.

2.5 Data source and acquisition. In silico studies were performed analyzing the publicly available dataset TCGA (The Cancer Genome Atlas). The mRNA expression data (RNA Seq V2 RSEM) and the patient information of the TCGA Invasive BC Cohort were retrieved from UCSC Xena (https://xenabrowser.net/) on the 22th December 2022. Samples (n. 1247) were filtered for missing values and by "sample type" in order to separate tumor tissues (n. 1104) from the adjacent normal tissues (n. 113). Furthermore, BC patients were classified on the basis of the presence or absence of the estrogen receptor (ER) detected by immunohistochemistry or according to the intrinsic molecular subtypes.

2.6 Survival analysis. The survival analyses were performed using the TCGA gene expression data along with the disease specific survival (DSS), overall survival (OS) or progression free interval (PFI) information. The survivALL package was employed in R Studio (version 4.1.3) to examine Cox proportional hazards for all possible points of separation (low-high cut-points), selecting the cut-point with the lowest p-value (54). Therefore, patients were divided according to high and low expression levels of specified genes. The Kaplan Meier survival curves were generated using the survival and the survminer packages in R Studio.

2.7 Enrichment and correlation analyses. In order to investigate the biological significance of the DEGs arising from the RNA-seq analysis, which display a log2FC ≥ 0.5 and p-value < 0.05, gene

ontology (GO) analysis was performed employing the *gseGO()* function of the topGO package (55) in R Studio. p-value ≤ 0.01 was considered as a significant threshold. The Pearson correlation coefficients (r-values) between the expression levels of EphA3 and the other genes of the TCGA (n. 20530) dataset were assessed in R Studio using the *cor.test()* function and setting the method as "Pearson". The statistical significance of the correlation coefficients was calculated by the t-test, $p < 0.001$ was considered as a cut-off criterion. The first 1000 positively correlated genes were selected for the next evaluations. In particular, aiming to cluster these genes in pathways and GO terms, we uploaded our list on the Database for Annotation, Visualization and Integrated Discovery (DAVID) functional annotation analysis website (https://david.ncifcrf.gov/). We grouped the genes in pathways by the option Kyoto Encyclopedia of Genes and Genomes (KEGG); furthermore, we clustered the genes by the Gene Ontology tool and the options GOTERM_BP, GOTERM_MF, GOTERM_CC. In both analyses the official gene symbol as "select identifier" and gene list as "list type" were chosen in the options of the upload and a limit species of "Homo sapiens" in the background was selected.

2.8 Gene silencing experiments. Silencing of EphA3 and RAGE was performed by transiently transfecting the cells for 36 h using Lipofectamine RNAiMAX (Thermo Fisher Scientific). Cells were seeded in six-well multi-dishes and transiently transfected after 24 h with a pool of three unique 27mer siRNA duplexes targeting-sequences (siEPHA3 or siAGER) or a non-targeting scramble control (OriGene Technologies, DBA, Milan, Italy).

2.9 Gene expression studies. Total RNA was extracted, and cDNA was synthesized by reverse transcription as previously described (48). The expression of selected genes was quantified by real-time PCR using platform Quant Studio7 Flex Real-Time PCR System (Thermo Fisher Scientific). Gene-specific primers were designed using Primer Express version 2.0 software (Applied Biosystems) and are as follows: 5′-CAGCGGCAGTAGCAATTATTCTC-3′ (EPHA3 forward) and 5′-CCACAGAACCTCCCAATCAAA-3′ (EPHA3 reverse); 5′-GTGAGAAGGGACTCCGTGTG-3′ (EFNB2 forward) and 5′-TAGACCCCAGAGGTTAGGGC-3′ (EFNB2 reverse); 5′-

AAGCCACCCCACTTCTCTCTAA-3′ (ACTB forward) and 5′- CACCTCCCCTGTGTGGACTT-3′ (ACTB reverse). Assays were performed in triplicate and the results were normalized for ACTB expression and then calculated as fold induction of RNA expression.

2.10 Chromatin Immunoprecipitation (ChIP) assay. Cells were grown in 10-cm dishes, then cross-linked with 1% formaldehyde and sonicated. Supernatants were immuno-cleared with salmon DNA/protein A-agarose (Merck Life Science) and immunoprecipitated with anti-Sp1 primary antibody (1C6, Santa Cruz Biotechnology) or nonspecific IgG. Pellets were washed, eluted with a buffer consisting of 1% SDS and 0.1 mol/L NaHCO3, and digested with proteinase K. DNA was obtained by phenol/chloroform extractions and precipitated with ethanol. The yield of target region DNA in each sample after ChIP was analyzed by real-time PCR. The primers used to amplify a region containing a Sp1 site located into the EphA3 promoter sequence were: 5′-CAAACTTGACATCAGCCTGCG-3′ (forward) and 5′-TCTCCATGAAGCATGCCACT-3′ (reverse). Data were normalized to the input for the immunoprecipitation and the results were reported as fold changes with respect to nonspecific IgG. The Sp1 sites within the EphA3 promoter were identified using the program "AliBaba2.1", which is a specific tool for predicting binding sites of transcription factors in an unknown DNA sequence by constructing matrices on the fly from TRANSFAC 4.0 sites.

2.11 Flow cytometry analysis. Cells (2×10^6) were fixed in ice-cold methanol for 10 min, permeabilized in 0.1% Triton X-100 in PBS for 15 min and incubated with primary antibody anti-RAGE (MAB1145, R&D Systems) for 1 h at 4°C. Alexa Fluor 488-conjugated secondary antibody (Thermo Fisher Scientific) was subsequently applied for another 30 min in the dark. Samples were then analyzed with CytoFLEX flow cytometry (Beckman-Coulter, Milan, Italy).

2.12 Western blot analysis. Cells were grown in 10-cm dishes, exposed to treatments where required and then lysed as previously described (56). Equal amounts of whole-protein extract were resolved on a 8-10% SDS-polyacrylamide gel and transferred to a nitrocellulose membrane (Amersham

Biosciences, Merck Life Science), which was probed with primary antibodies against RAGE (MAB1145, R&D Systems, 1:1000), EphA3 (12480-1-AP, Proteintech, 1:500), SP1 (1C6, Santa Cruz Biotechnology, 1:1000) and β-actin (AC-15, Santa Cruz Biotechnology, 1:4000) and then revealed using the Clarity™ Western ECL Substrate (Bio-Rad).

2.13 Immunofluorescence microscopy. Cells were grown on a cover slip, next were fixed in 4% paraformaldehyde in PBS, permeabilized with 0.2% Triton X-100, washed 3 times with PBS and incubated at 4 °C overnight with primary antibodies against RAGE (MAB1145, R&D Systems, 1:500) or Ephrin A3 (12480-1-AP, Proteintech, 1:100. After incubation, the slides were extensively washed with PBS, probed with Alexa Fluor 488 goat anti-mouse IgG or Alexa Fluor 555 goat anti-rabbit IgG (Thermo Fisher Scientific, 1:250) and 4′,6-diamidino-2-phenylindole dihydrochloride (DAPI) (Merck Life Science, 1:1000). Images were obtained using the EVOS™ M7000 Imaging System (Thermo Fisher Scientific) and analyzed using ImageJ software by selecting one cell at a time in each picture and measuring the area, integrated density and mean gray value. Thereafter, the corrected total cell fluorescence (CTCF) = integrated density - (area of selected cell × mean fluorescence of background readings) was calculated. Box plots and statistical analysis (t-tests) were performed using R Studio.

2.14 Scanning Electron Microscopy. Cells were fixed in 3% glutaraldehyde in 0.1 M phosphate buffer (pH 7.2) for 2 h at 4°C, washed three times with 0.1 M phosphate buffer, pH 7.2, and post-fixed in 1% osmium tetroxide in the same buffer. After 2 h, the samples were dehydrated using increasing concentrations of ethanol and dried with hexamethyldisilazane. Finally, glass slides were mounted on standard aluminum stubs with double-sided conductivity tape, coated with carbon, and observed at various magnifications using the Ultra High Resolution SEM (UHR-SEM) – ZEISS CrossBeam 350.

2.15 Colony formation assay. Cells were cultured in regular growth medium to 90% confluence. Cells were then trypsinized, counted and seeded (3×10^3) in six-well plates in medium containing

2.5% charcoal-stripped FBS. Media were renewed every 2 days. After 10 days, cells were washed with PBS, fixed in acetone:methanol (1:1) for 3 min at room temperature and then stained with Giemsa for 10 min. A total of 10 pictures for each condition was detected using a digital camera and colony number (more than 40 cells) was measured by ImageJ program.

2.16 Migration and invasion assays. Transwell 8 μm polycarbonate membranes (Costar, Merck Life Science) were used to evaluate *in vitro* cell migration and invasion. 5×10^4 cells (previously transfected where required) in 300 μL serum-free medium were seeded in the upper chamber coated with (invasion assay) or without (migration assay) Corning® Matrigel® Growth Factor Reduced (GFR) Basement Membrane Matrix (Merck Life Science) (diluted with serum-free medium at a ratio of 1:3). Medium containing 2.5% FBS and treatments was added to the bottom chambers. 18 h after seeding, cells on the upper surface of the membrane were then removed by wiping with Q-tip, and migrated or invaded cells were fixed with 100% methanol, stained with Giemsa (Merck Life Science), photographed using an inverted phase contrast microscope and counted using the WCIF ImageJ software.

2.17 Co-culture Matrigel drops evasion assay. The Matrigel drop assay was performed as previously described (57, 58). 5×10^4/drop of MCF7/wt or MCF7/RAGE cells and CAFs (ratio 2:1) were gently mixed with 10 μl of Corning® Matrigel® Growth Factor Reduced (GFR) Basement Membrane Matrix (Merck Life Science). The cell/matrigel suspension was layered onto the surface of 24-well plate to form a well-defined drop and placed at 37 °C to solidify. Medium containing vehicle or 10 μM AWL-II-38.3 was then placed over the drop. Cells were observed at specified time points and drops were photographed using the EVOS™ M7000 Imaging System (Thermo Fisher Scientific). The migrating edge outside the Matrigel drop was measured with ImageJ software.

2.18 Zebrafish maintenance and egg collection. Wild-type adult zebrafish (6-8 months) of both sexes were purchased from a local store and maintained in 100 L aquaria filled with aged tap water (temperature 28±0.5°C, pH 7.3, conductivity 300 L/cm, dissolved oxygen 8±1 mg/L, hardness 180

mg, 14 h light/10 h dark photoperiod). Embryos obtained from the spontaneous spawning of adult fish were collected within 2 hours and staged as previously reported (59). Fertilized healthy embryos were maintained in Petri dishes containing aged tap water in a 28.5°C incubator.

2.19 Zebrafish microinjections. At 48 hours post-fertilization (hpf), dechorionated larvae were anesthetized with tricaine methanesulphonate (MS-222) and positioned on a modified Petri dish coated with 1.5% w/v agarose. Before injection, cells were labeled *in vitro* with CellTracker™ CM-DiI Dye (Thermo Fisher Scientific). Approximately 250 cells were resuspended in a complete medium, and 33.51 nL of cell solution were injected using commercially available ready-to-use tip needles (15 μm inner diameter, Eppendorf, Germany) into the yolk sac. An Eppendorf's semi-automated microinjection system equipped with the micromanipulator InjectMan 4 connected to FemtoJet 4x was used for the injections, with an injection pressure of 100 hPa, 0.2 sec injection time and 20 hPa of compensation pressure. After injections, the larvae were immediately transferred into housing-keeping water. Injected larvae were kept at 28±0.5°C and examined every other day for monitoring tumor growth and invasion using the EVOS™ M7000 Imaging System (Thermo Fisher Scientific).

2.20 Statistical analysis. All bioinformatics analyses were carried out using R Studio. The volcano plots were performed with the tidyverse package. Box plots were performed with the tidyverse package and the related statistical analysis was performed using the Wilcoxon test. Statistical analysis was performed using t-tests.

3.RESULTS

3.1 RAGE triggers a transcriptional gene signature toward BC cell motility. On the basis of previous evidence showing the involvement of RAGE in BC progression (60, 36), we first explored its clinical significance in the cohort of BC patients of the TCGA database. We have found that high expression levels of RAGE correlate with a worse progression free interval (PFI) in ER-positive (Fig. 3.1.1 A) but not in ER-negative (data not shown) BC patients.

Therefore, we engineered MCF7 and T47D ER-positive BC cells to stably overexpress RAGE (MCF7/RAGE and T47D/RAGE) to provide novel insights into the role of RAGE in ER-positive BC. First, microscopic evaluation showed that both MCF7/RAGE and T47D/RAGE cells exhibit a spindle-shaped phenotype with membrane protrusions compared to MCF7 and T47D wild type (MCF7/wt and T47D/wt) cells (Fig.3.1.1 B e Fig.3.1.1 C). Flow cytometry analyses and immunoblotting experiments confirmed that significative increased RAGE protein levels characterize RAGE-overexpressing (MCF7/RAGE and T47D/RAGE) cells respect to MCF7/wt and T47D/wt cells (Fig.3.1.1 D-G).

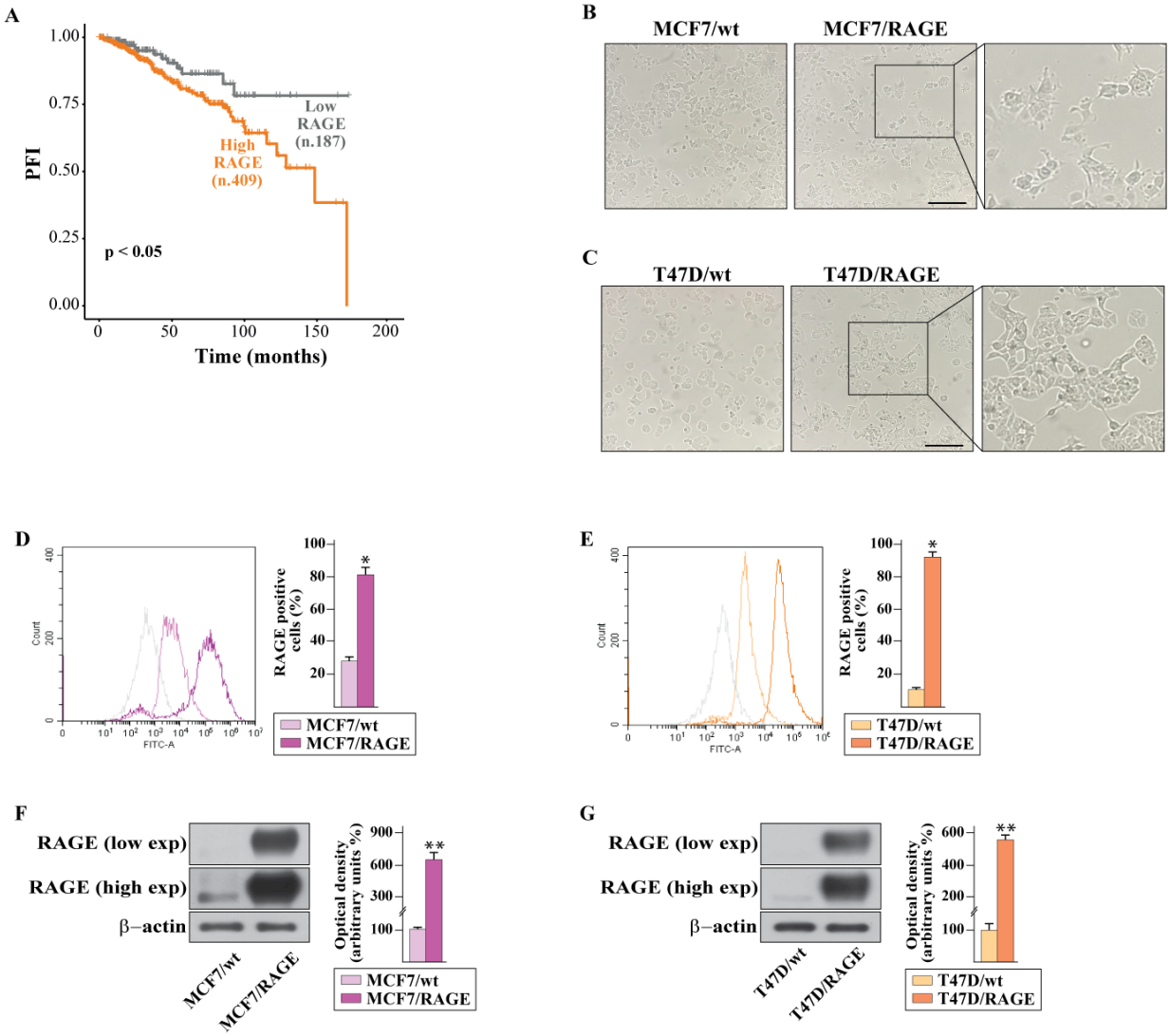

Fig.3.1.1 Validation of RAGE-overexpressing BC cells. (A) Kaplan-Meier plot showing the association of RAGE mRNA expression with the progression free interval (PFI) of the TCGA ER-positive BC patients. Samples were divided into RAGE high and low groups using the optimum cut-off. (B-C) Morphological appearance of wild type (MCF7/wt and T47D/wt) and RAGE-overexpressing (MCF7/RAGE and T47D/RAGE) cells in phase-contrast microscopy; scale bar: 250 µm. Enlarged details are shown in the separate boxes. Flow cytometric histograms in RAGE-overexpressing compared with wild type MCF7 (D) and T47D (E) cells. FITC, fluorescein isothiocyanate. Side panels show the percentage of RAGE-positive cells. (F-G) Immunoblots of RAGE in wild type (MCF7/wt and T47D/wt) and RAGE-overexpressing (MCF7/RAGE and T47D/RAGE) cells. Side panels show densitometric analysis of the blots normalized to β-actin, which was used as a loading control. Values represent the mean ± SD of three independent experiments performed in triplicate.

Similar results were obtained performing immunofluorescence experiments, as shown in the figure 3.1.2.

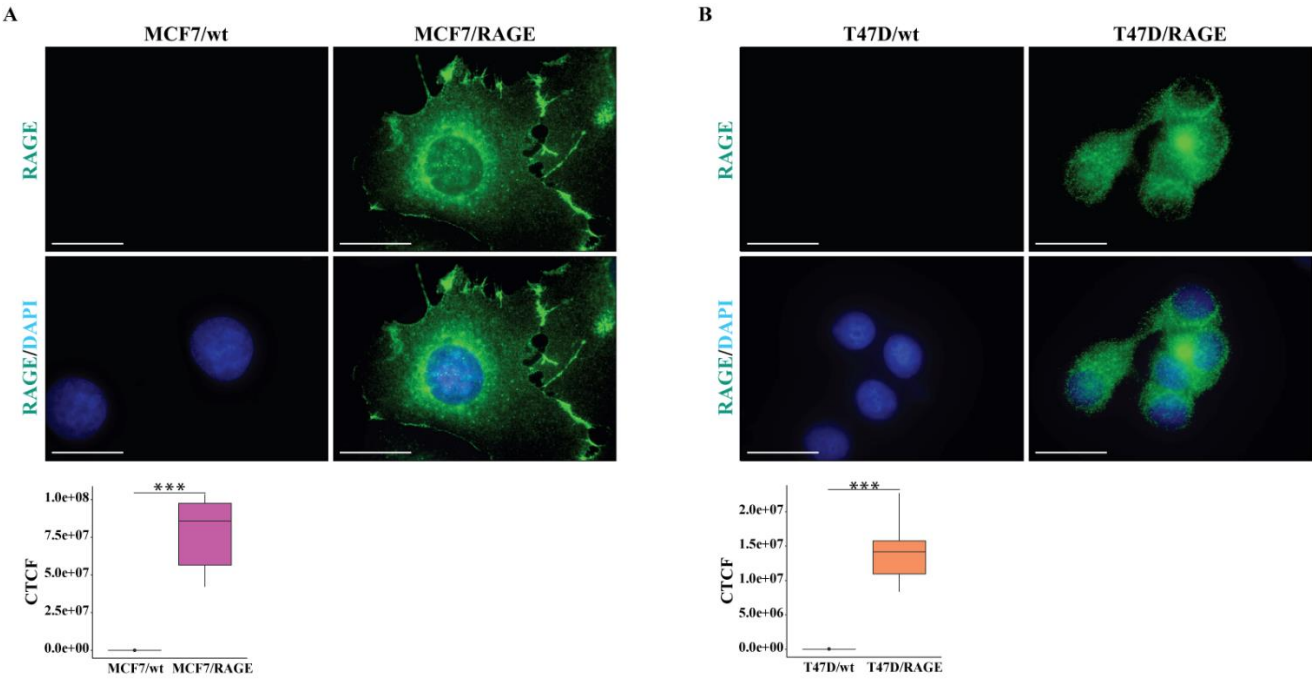

Fig.3.1.2 Validation of RAGE-overexpressing by immunofluorescence assay (A-B) Evaluation of RAGE protein expression (green signal) by immunofluorescence experiment in wild type (MCF7/wt and T47D/wt) and RAGE-overexpressing (MCF7/RAGE and T47D/RAGE) cells; nuclei were stained by DAPI (blue signal). The images shown represent 10 random fields from three independent experiments. Scale bar: 25 μm. Side panels represent corrected total cell fluorescence (CTCF), which was calculated on at least 10 pictures from each sample. (*) indicates $p < 0.05$; (**) indicates $p < 0.01$; (**) indicates $p < 0.001$

In order to appreciate the whole transcriptomic landscape regulated by RAGE in ER-positive BC cells, we performed RNA sequencing (RNA-seq) analysis in MCF7/wt and MCF7/RAGE cells. Figure 3.1.3 (panel A) shows the volcano plot portraying the differentially expressed genes (DEGs) in MCF7/RAGE respect to MCF7/wt cells. In particular, 725 genes were found up-regulated ($\log2FC \geq 0.5$, $p < 0.05$) and 1340 genes were found down-regulated ($\log2FC \leq -0.5$, $p < 0.05$) in MCF7/RAGE respect to MCF7/wt cells. To ascertain the biological role of the up-regulated DEGs in RAGE-overexpressing BC cells, we performed gene ontology (GO) analysis by clustering these genes according to biological process (BP), molecular function (MF) and cellular component (CC) terms. We found that “cell-cell adhesion”, “chemotaxis”, “biological adhesion” and “cell adhesion” are the

most significantly enriched BP terms (Fig. 3.1.3 A, side box). Thereafter, in order to explore whether the genes of the aforementioned BP terms, which of note include also RAGE (AGER, gene symbol) (Fig. 3.1.3 B) may have a prognostic value in ER-positive BC patients, we took advantage of the TCGA database. For the subsequent analyses, we employed the "biological adhesion" set of genes as it includes all the genes belonging to the "cell-cell adhesion" and "cell adhesion" terms. Interestingly, the cumulative expression of the chemotaxis-related genes (Fig.3.1.3 C) or the biological adhesion genes (Fig.3.1.3 D) is associated with a worse disease specific survival (DSS) in ER-positive BC patients, as revealed by the Kaplan-Meier survival plots shown. These findings indicate that RAGE may drive transcriptional changes associated with increased motility in ER-positive BC cells.

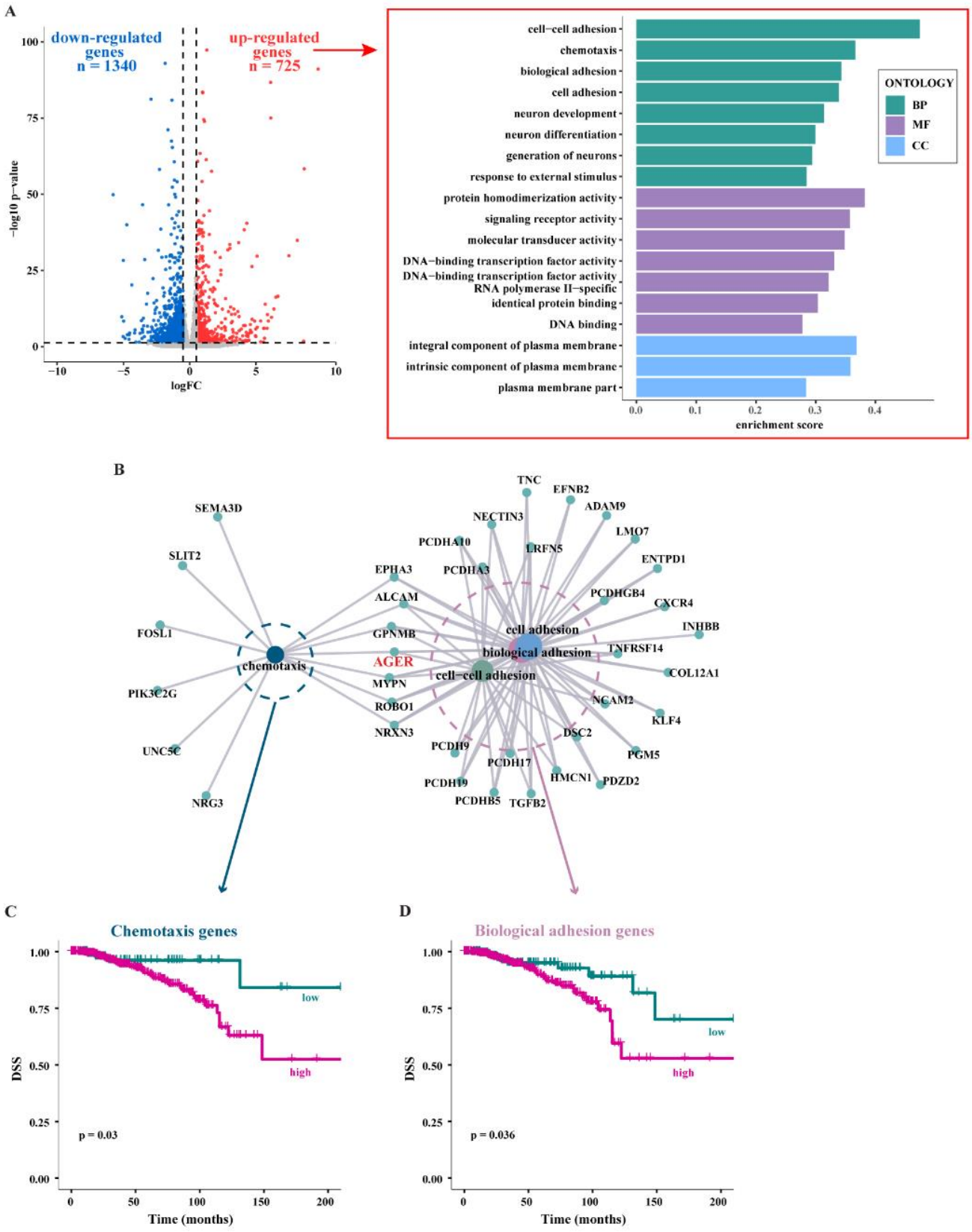

Fig.3.1.3 Comprehensive transcriptome analysis by RNA-seq of wild type and RAGE-overexpressing MCF7 cells. (A) Volcano plot evidencing the differentially expressed genes (DEGs)

in RAGE-overexpressing (MCF7/RAGE) respect to wild type (MCF7/wt) MCF7 cells, as ascertained by RNA-seq analysis. p-value < 0.05 was considered as a significant threshold; significantly down-regulated genes (log2FC ≤ 0.5 and p < 0.05) are shown in blue (n = 1340), significantly up-regulated genes (log2FC ≥ 0.5 and p < 0.05) are shown in red (n = 725), non-significant genes are shown in grey (p > 0.05). Side box shows enrichment scores for gene ontology (GO) terms of the up-regulated DEGs in MCF7/RAGE versus MCF7/wt cells, involved in biological process (BP), molecular function (MF), cellular component (CC), according to p < 0.05 and log2FC > 0.5. (B) Interrelation analysis of "cell-cell adhesion", "chemotaxis", "biological adhesion" and "cell adhesion" BP and relative genes. Survival analysis showing the association of high expression of the genes belonging to the "chemotaxis" (C) and "biological adhesion" (D) BP with a worse disease specific survival (DSS) in ER-positive BC patients of the TCGA cohort.

3.2 RAGE overexpression stimulates the dissemination potential in BC cells. Based on the RNA-seq results, morphological and functional studies were performed in RAGE-overexpressing BC cells. Scanning electron microscopy (SEM) revealed that increased RAGE levels stimulate many cytoplasmic protrusions, known as filopodia, in MCF7/RAGE and T47D/RAGE respect to wild type cells (Fig. 3.2.1 A-D).

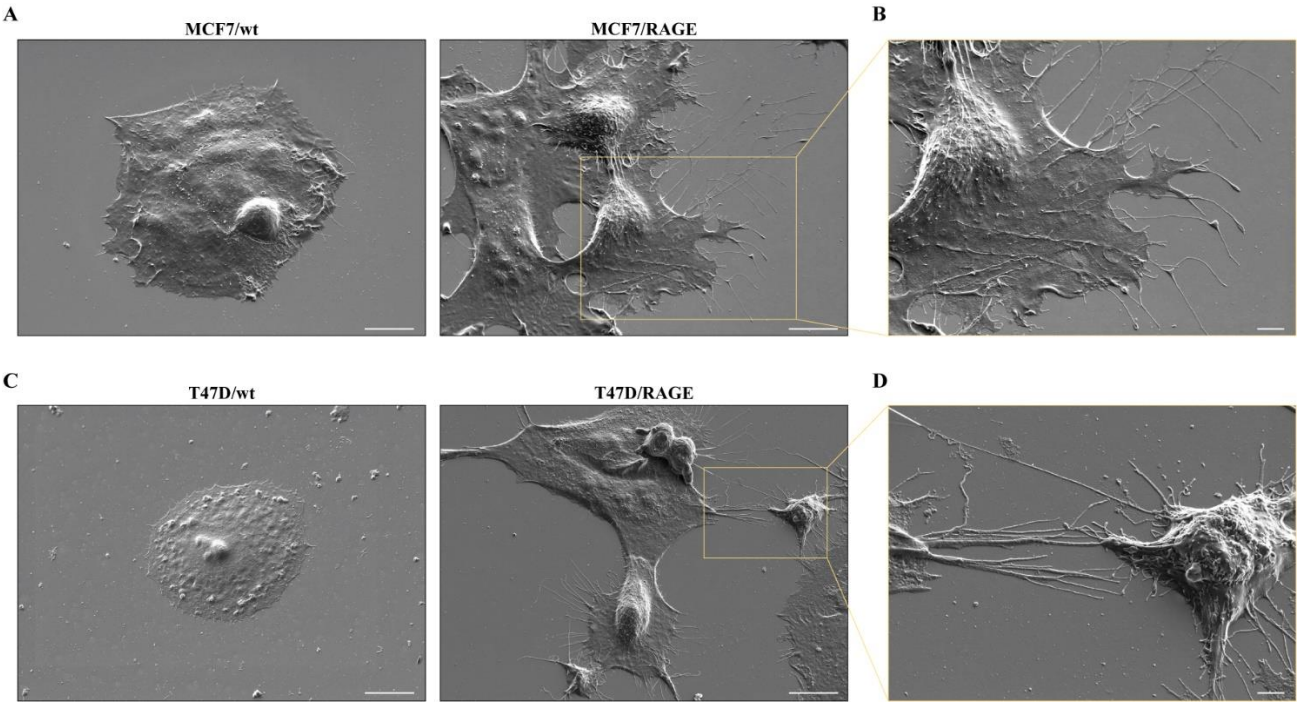

Fig.3.2.1 Membrane protrusions in RAGE-overexpressing BC cells. (A) Scanning electron microscopy (SEM) images of wild type (MCF7/wt) and RAGE-overexpressing (MCF7/RAGE) MCF7 cells; scale bar: 10 μm. (B) Higher magnification (square in A), scale bar: 3 μm. (C) SEM

images of wild type (T47D/wt) and RAGE-overexpressing (T47D/RAGE) T47D cells; scale bar: 10 μm. (D) Higher magnification (square in C), scale bar: 2 μm.

Based on these findings and in accordance with previous evidence indicating that the presence of filopodial protrusions play a pivotal role in cell motility (61, 62), we found that MCF7/RAGE and T47D/RAGE cells display a higher migratory (Fig.3.2.2 A-B) and invasive (Fig.3.2.2 C-D) potential compared to MCF7/wt and T47D/wt cells, respectively.

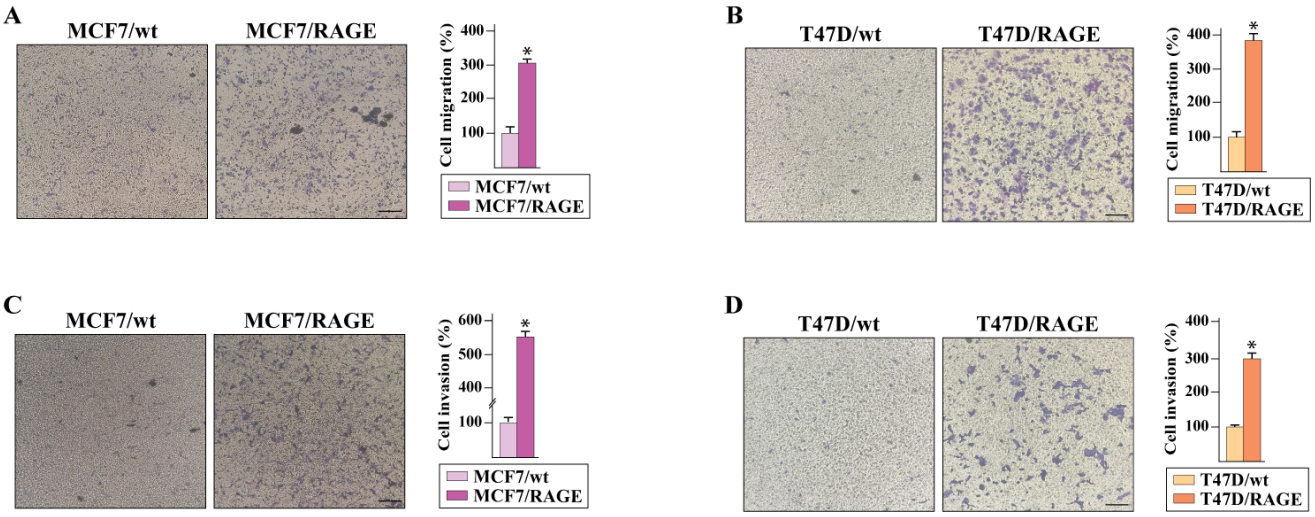

Fig.3.2.2 Migration and invasion in RAGE-overexpressing BC cells. Transwell migration (A-B) and invasion (C-D) assays in wild type and RAGE-overexpressing MCF7 and T47D cells. Cells were counted in at least 5 random fields in three independent experiments performed in triplicate, as quantified in the side panels. Scale bar 200 μm.

Worthy, the migratory (Fig.3.2.3 A-B) and invasive (Fig.3.2.3 C-D) behavior of RAGE-overexpressing BC cells was weakened after silencing RAGE expression by a specific siRNA (Fig.3.2.3E-F), thus suggesting the involvement of RAGE in facilitating a motile phenotype in BC cells.

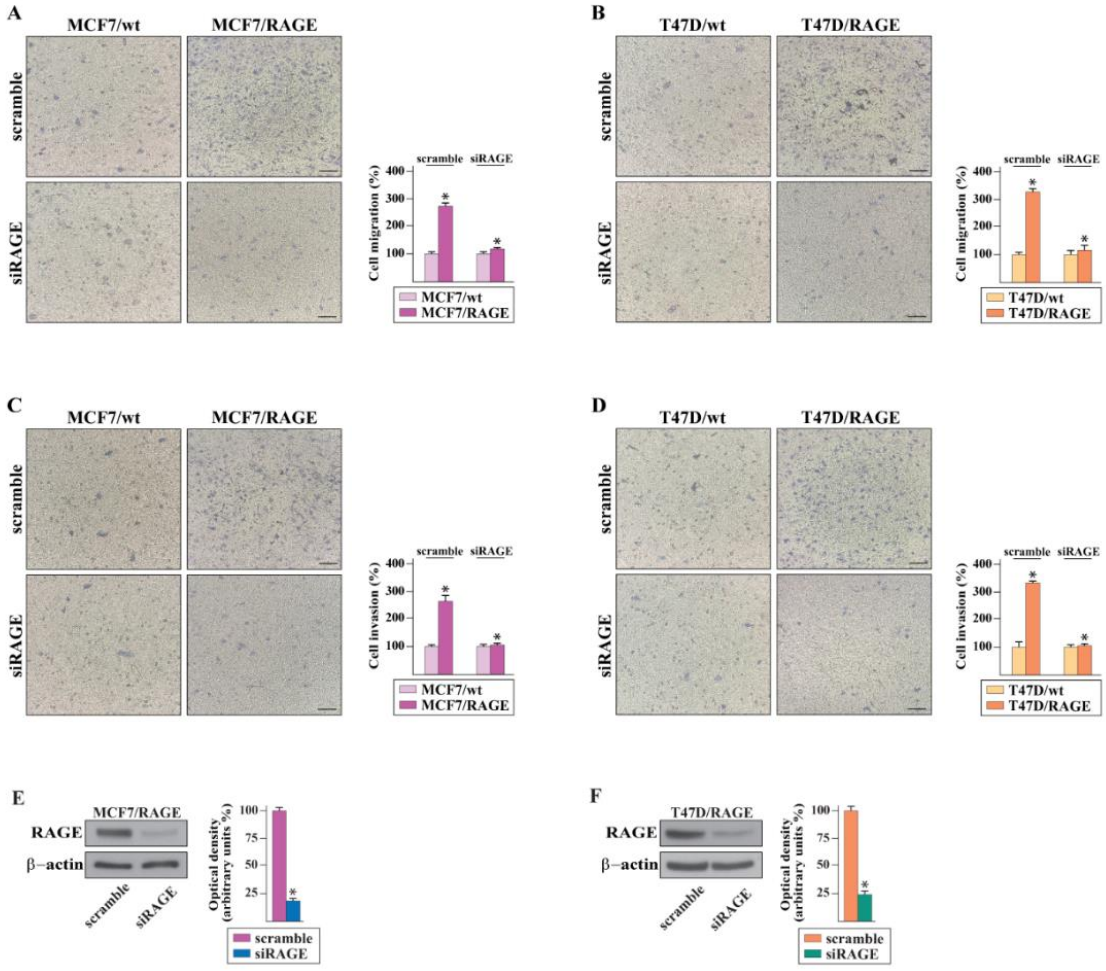

Fig.3.2.3 RAGE silencing impairs the migratory and invasive behavior of RAGE-overexpressing BC cells. Transwell migration (A-B) and invasion (C-D) assays in wild type and RAGE-overexpressing MCF7 and T47D cells. Cells were counted in at least 5 random fields in three independent experiments performed in triplicate, as quantified in the side panels. Scale bar 200 μm. Efficacy of RAGE silencing in MCF7/RAGE (E) and T47D/RAGE (F) cells. Side panels show densitometric analysis of the blots normalized to β-actin, which was used as a loading control. Results shown are representative of at least three independent experiments. (*) indicates $p < 0.05$.

Next, we also performed colony formation assays in order to assess the ability of RAGE-overexpressing MCF7 and T47D cells to form colonies. The results obtained indicate that the clonogenic potential of RAGE-overexpressing cells significantly increase compared to MCF7/wt and T47D/wt cells (Fig.3.2.4 A-B). Then, we turned to an *in vivo* model system in order to investigate the role of RAGE in promoting early events of the metastatic cascade. To this aim, cells were labeled with DiI dye and injected into the yolk sac of 48-hour post-fertilization (hpf) zebrafish larvae. After 3 days, we observed that tumor growth increased in zebrafish xenotransplanted with RAGE-overexpressing cells compared to wild-type cells (Fig.3.2.4 C-D, F-G). Fascinatingly, MCF7/RAGE (Fig.3.2.4 C, E) and T47D/RAGE (Fig.3.2.4 F, H) cells were able to spread into the zebrafish dorsal stripe, while MCF7/wt and T47D/wt xenotransplanted groups did not show significant evidence of metastases (Fig.3.2.4 C, E, F, H), in accordance with previous findings (63, 64).

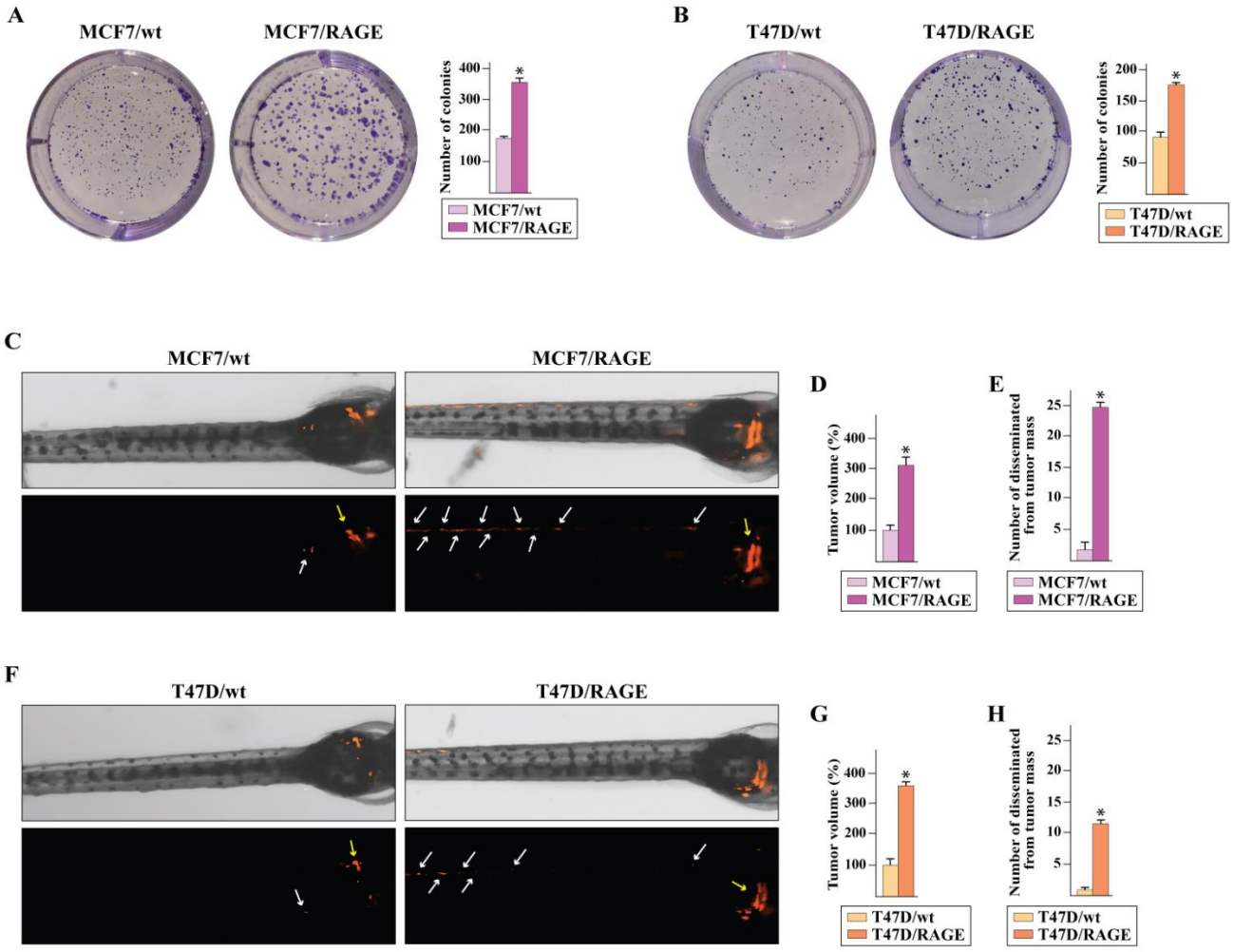

Fig 3.2.4 Proliferative and metastatic dissemination of RAGE-overexpressing BC cells. (A-B) Colony formation in wild type (MCF7/wt and T47D/wt) and RAGE-overexpressing (MCF7/RAGE and T47D/RAGE) MCF7 and T47D cells. After 10 days of incubation cell colonies were stained and pictures were captured by a digital camera. Colonies were counted using the program WCIF ImageJ for Windows. Each data point is the mean ± SD of three independent experiments performed in triplicate. (C, F) DiI-labeled wild type (MCF7/wt and T47D/wt) and RAGE-overexpressing (MCF7/RAGE and T47D/RAGE) cells were injected into the yolk sac of 48 hpf larvae, and tumor cell growth and dissemination were detected using fluorescent microscopy at day 3 post-injection. Yellow arrows indicate primary tumors. White arrows indicate disseminated tumor foci. (D, G) Quantification of DiI-labeled tumor volume (n= 6/group). The mean value of the tumor size in wild type zebrafish xenografts was settled as 100%. (E, H) Quantification of numbers of disseminated tumor foci (n =6/group). Data are represented as mean ± SD. (*) indicates $p < 0.05$.

3.3 EphA3 mediates the RAGE-relied motile phenotype of BC cells. Next, we aimed to uncover the molecular mechanisms underlying the RAGE-mediated breast cancer growth and metastatic spread**.** The RNA-seq data showed that the receptor tyrosine kinase EphA3, which belongs to both biological adhesion and chemotaxis GO terms, is one of most up-regulated genes in MCF7/RAGE respect to MCF7/wt cells. In accordance with RNA-seq data and previous evidence showing the role of Eph receptors in regulating tumor growth, migration and invasion (63), we ascertained that RAGE-overexpressing BC cells exhibit a higher mRNA (Fig.3.3.1 A) and protein (Fig.3.3.1 B-E) expression of EphA3 respect to the parental counterparts.

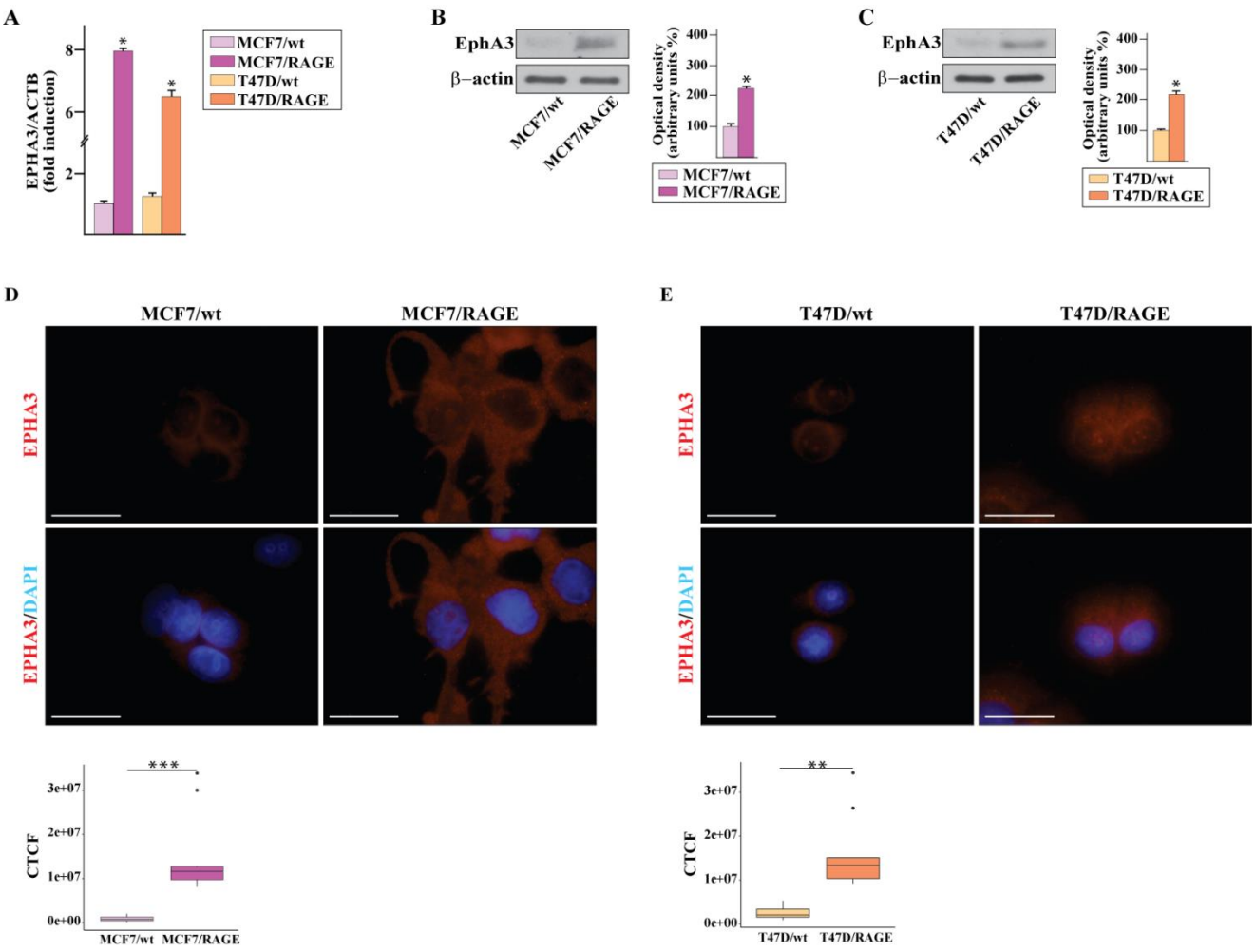

Fig.3.3.1. Up-regulation of Epha3 in RAGE-overexpressing BC cells. (A) mRNA expression of EPHA3 in RAGE-overexpressing (MCF7/RAGE and T47D/RAGE) respect to wild type (MCF7/wt and T47D/wt) cells, as ascertained by real-time PCR. Values are normalized to the actin beta (ACTB) expression and shown as fold changes of mRNA expression in RAGE-overexpressing respect to wild

type cells. (B-C) Immunoblots of EphA3 in wild type (MCF7/wt and T47D/wt) and RAGE-overexpressing (MCF7/RAGE and T47D/RAGE) cells. Side panels show densitometric analysis of the blots normalized to β-actin, which was used as a loading control. (D-E) Evaluation of EphA3 protein expression (red signal) by immunofluorescence experiment in wild type (MCF7/wt and T47D/wt) and RAGE-overexpressing (MCF7/RAGE and T47D/RAGE) cells; nuclei were stained by DAPI (blue signal). The images shown represent 10 random fields from three independent experiments. Bottom panels represent corrected total cell fluorescence (CTCF), which was calculated on at least 10 pictures from each sample. Scale bar: 25 μm.

Considering that MCF7/RAGE express higher levels of Sp1 than MCF7/wt cells, we investigated the role of this transcription factor in EphA3 regulation. First, we ascertained that three Sp1 sites are located within the promoter sequence of EphA3 (Fig.3.3.2 A). Next, we confirmed that Sp1 is up-regulated in both MCF7/RAGE and T47D/RAGE cells respect to wild type cells (Fig.3.3.2 B-C). In accordance with these results, the Sp1 inhibitor mithramycin A (MMA) showed the capacity to low EphA3 levels in RAGE-overexpressing BC cells (Fig.3.3.2 D-E), suggesting the involvement of Sp1 in EphA3regulation, as previously shown (66). Corroborating the role of Sp1 in the regulation of EphA3 in RAGE-overexpressing BC cells, we demonstrated by chromatin immunoprecipitation (ChIP) assays that Sp1 can be recruited to the EphA3 promoter region in both MCF7/RAGE and T47D/RAGE cells (Fig.3.3.2 F). Accordingly, the Sp1 inhibitor MMA prevented these effects (Fig.3.3.2 F).

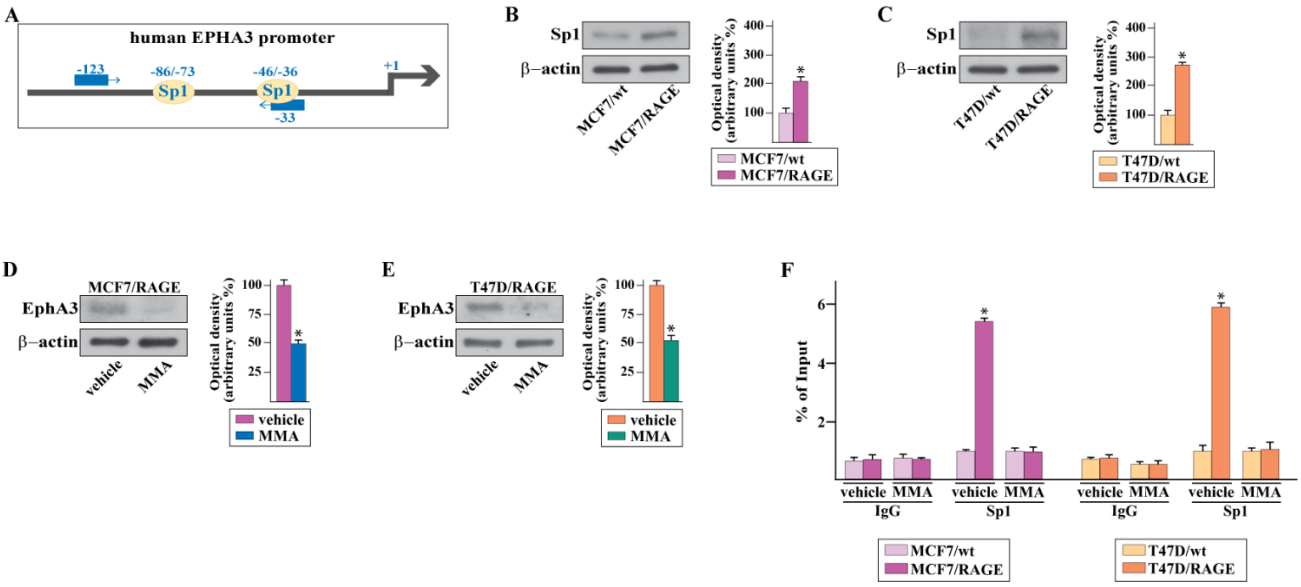

Fig.3.3.2 The transcription factor Sp1 is required for inducing Epha3 expression in RAGE-overexpressing BC cells. (A) Schematic representation of human EPHA3 promoter carrying the Sp1-responsive sites (the transcriptional start site is indicated as + 1). (B-C)) Protein expression of Sp1 in wild type (MCF7/wt and T47D/wt) and RAGE-overexpressing (MCF7/RAGE and T47D/RAGE) cells, as evaluated by immunoblotting. (D-E) Protein levels of EphA3 in the presence of 100 nM Sp1 inhibitor mithramycin A (MMA) in RAGE-overexpressing (MCF7/RAGE and T47D/RAGE) cells. Side panel shows densitometric analysis of the blots normalized to β-actin. (F) Recruitment of Sp1 to EphA3 promoter by ChIP assay in wild type (MCF7/wt and T47D/wt) and RAGE-overexpressing (MCF7/RAGE and T47D/RAGE) cells in the presence or absence of 100 nM Sp1 inhibitor mithramycin A (MMA). In control samples nonspecific IgGs were used instead of the primary antibody. The amplified sequences were evaluated by real-time PCR. Values represent the mean ± SD of three independent experiments performed in triplicate. (*) indicates $p < 0.05$

Eph receptors and their ligands ephrins may originate two different types of bidirectional signaling: the forward signal depends on the Eph kinase activity and propagate to cells that express the receptor, whereas the reverse signal is a result of the activation of Src kinases and propagate to ligand-expressing cells (65). In accordance with these evidences and taking into account our RNA-seq and real-time PCR data showing that MCF7/RAGE and T47D/RAGE cells express high levels of the EphA3 ligand namely Ephrin B2 (Fig 3.3.3), we performed migration and invasion assays in the presence of the EphA3 kinase inhibitor AWL-II-38.3, which prevents the kinase-dependent EphA3 forward signaling.

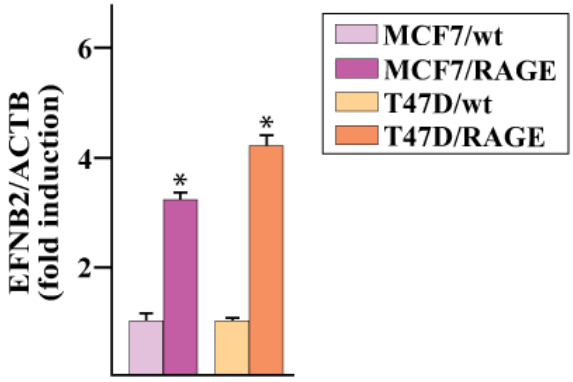

Fig.3.3.3 Analysis of the expression of Ephrin B2 in wild type and RAGE-overexpressing MCF7 cells. mRNA expression of Ephrin B2 in RAGE-overexpressing (MCF7/RAGE) respect to wild type (MCF7/wt) cells, as ascertained by real-time PCR. Values are normalized to the actin beta (ACTB) expression and shown as fold changes of mRNA expression in RAGE-overexpressing respect to wild type cells. Values represent the mean ± SD of three independent experiments performed in triplicate. (*) indicates $p < 0.05$.

Having determined that AWL-II-38.3 is not able to modify the protein levels of EphA3 (Fig. 3.3.4), we observed that it is able to reduce the migratory (Fig. 3.3.5 A-B) and invasive (Fig. 3.3.5 C-D) capabilities of RAGE-overexpressing.

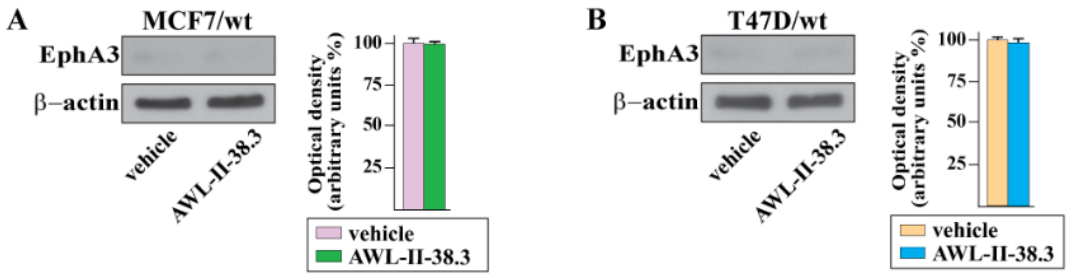

Fig.3.3.4 The EphA3 inhibitor AWL-II-38.3 does not modify the whole protein levels of EphA3. Immunoblots of EphA3 in MCF7/RAGE (A) and T47D/RAGE (B) cells in the presence or absence of the EphA3 inhibitor AWL-II-38.3. Side panels show densitometric analysis of the blots normalized to β-actin, which was used as a loading control. Values represent the mean ± SD of three independent experiments performed in triplicate.

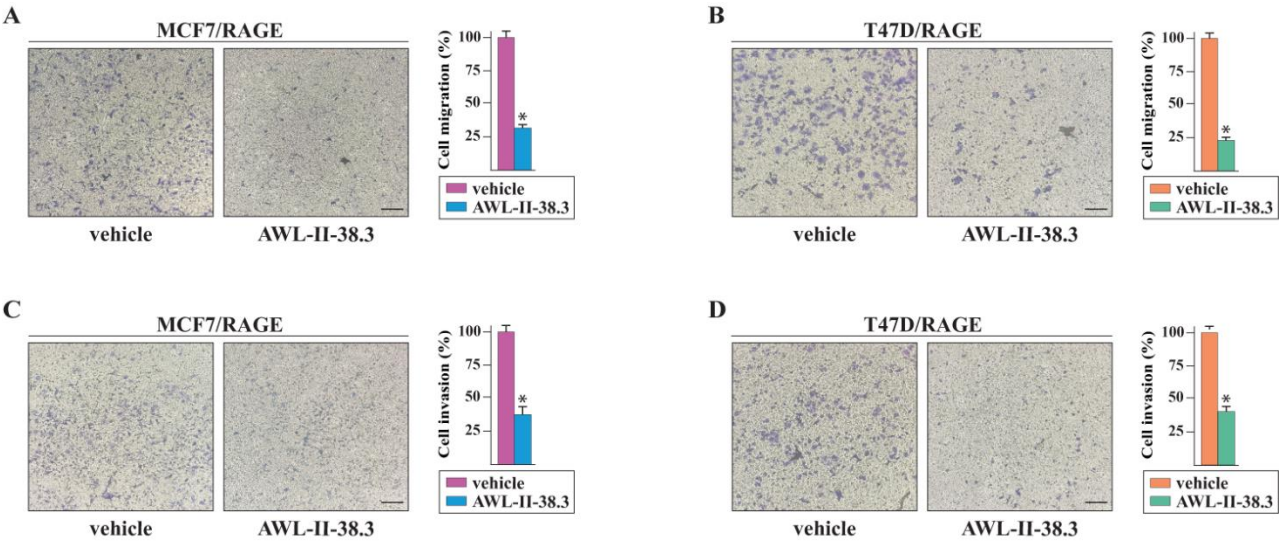

Fig.3.3.4 The EphA3 inhibitor AWL-II-38.3 reduce the migration and inasivasion of BC cells. Transwell migration (A-B) and invasion (C-D) assays in MCF7/RAGE and T47D/RAGE cells in the presence or absence of 10 μM EphA3 inhibitor AWL-II-38.3. Cells were counted in at least 5 random fields in three independent experiments performed in triplicate, as quantified in the side panels. Scale bar: 200 μm. Values represent the mean ± SD of three independent experiments performed in triplicate. (*) indicates $p < 0.05$.

In accordance with these findings, we ascertained that the migration and invasion of MCF7/RAGE and T47D/RAGE cells is abrogated after silencing EphA3 expression. Overall, these data indicate that EphA3, particularly its forward signal, may play a critical role in the migration and invasion observed in RAGE-overexpressing BC cells (Fig.3.3.6 A-F).

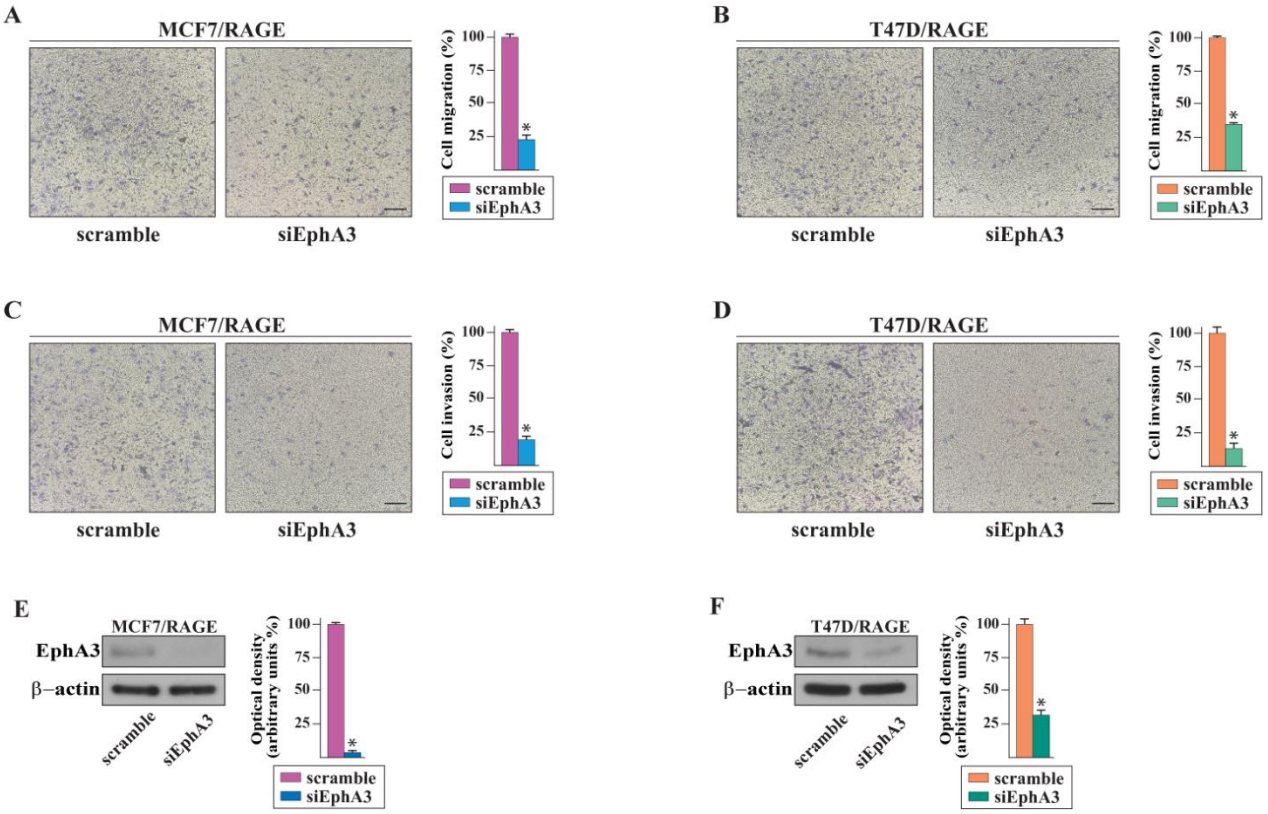

Fig.3.3.6 The EphA3 forward signal is involved in the migration and invasion of RAGE-overexpressing BC cells. Transwell migration (A-B) and invasion (C-D) assays in MCF7/RAGE and T47D/RAGE cells in the presence or absence of EphA3 silencing. Efficacy of EphA3 silencing in MCF7/RAGE (E) and T47D/RAGE (F) cells. Side panel shows densitometric analysis of the blots normalized to β-actin.

Next, we aimed to explore the clinical significance of EphA3 in BC taking advantage of the TCGA cohort of BC samples. Our analysis indicated that the levels of EphA3 are more elevated in ER-positive respect to ER-negative BC patients (Fig. 3.3.7 A) as well as in the luminal compared to the other molecular subtypes (Fig.3.3.7 B). Moreover, increased EphA3 levels were found to be significantly associated with a worse overall survival (OS) (Fig.3.3.7 C) and DSS (Fig.3.3.7 D) in ER-positive BC patients. Furthermore, we ascertained that elevated EphA3 levels may be predictive of a worse OS in BC patients displaying high RAGE levels (Fig.3.3.7 E).

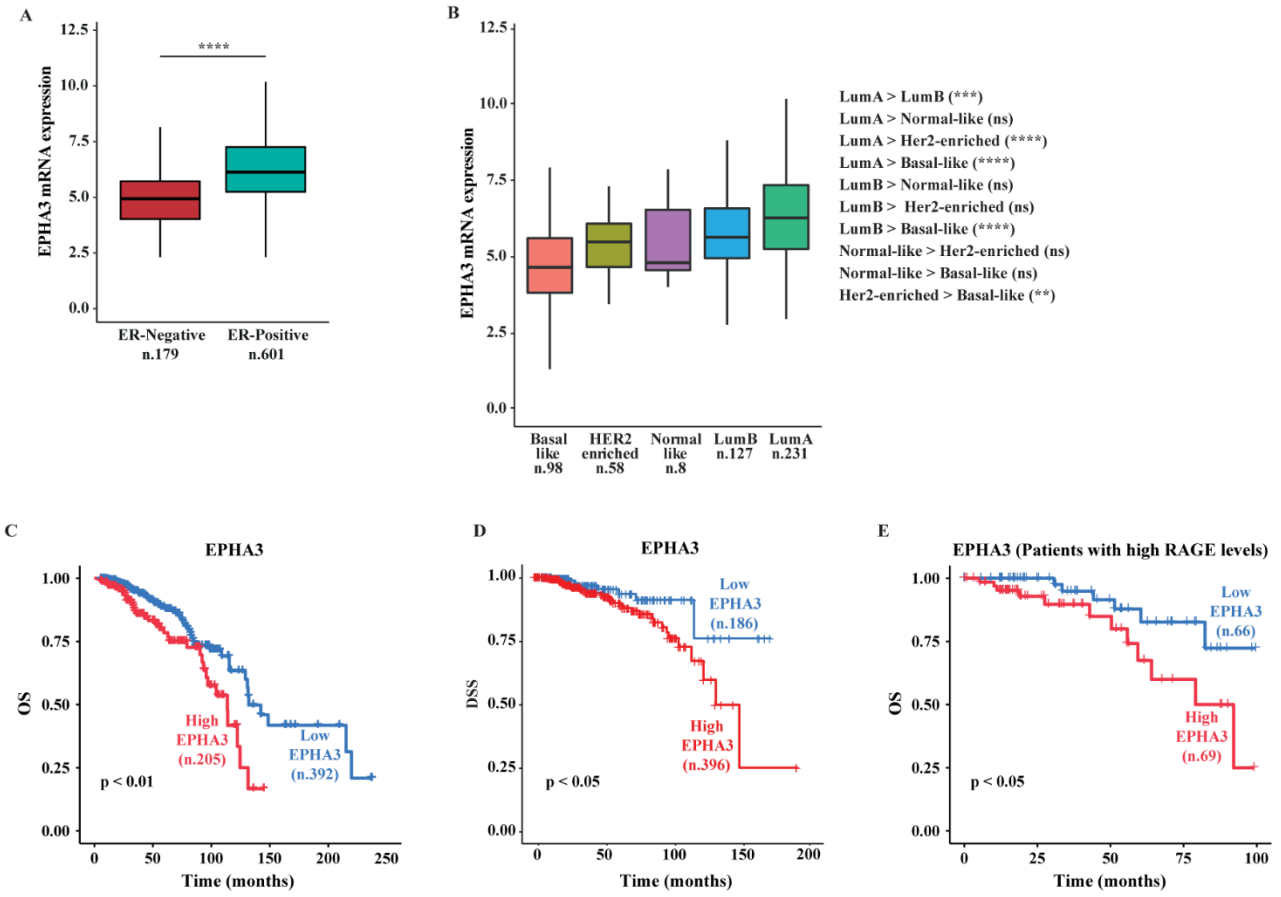

Fig.3.3.7 EphA3 expression correlates with poor clinical outcomes in ER-positive BC patients. (A) Box plot showing the differential EphA3 expression levels in ER-positive and negative BC patients, as found in the TCGA dataset. (B) EphA3 mRNA levels according to BC intrinsic molecular subtypes of the TCGA cohort. The number of patients is reported in each panel. Kaplan-Meier plots showing the association of EphA3 expression with the overall survival (OS) (C) and disease specific survival (DSS) (D) of the TCGA ER-positive BC patients. Patients were divided into EphA3 high and low categories using the optimum cut-off. (E) Kaplan-Meier plot showing the association of EphA3 expression with the OS of ER-positive BC patients characterized by high RAGE expression levels (above the 3Q). Patients were divided into EphA3 high and low categories using the optimum cut-off.

Afterward, we used the top 1000 EphA3-correlated genes, ranked by Pearson correlation coefficients, to perform KEGG pathway enrichment and GO analyses in ER-positive BC patients. The EphA3-related genes were found to be associated with both transduction pathways (Fig.3.3.8 A) and GO terms (Fig.3.3.8 B-D) implicated in the migratory and invasive ability of BC cells. These findings show that RAGE may contribute to an aggressive behavior of BC cells by driving an EphA3-dependent transcription of genes that promote BC cell motility.

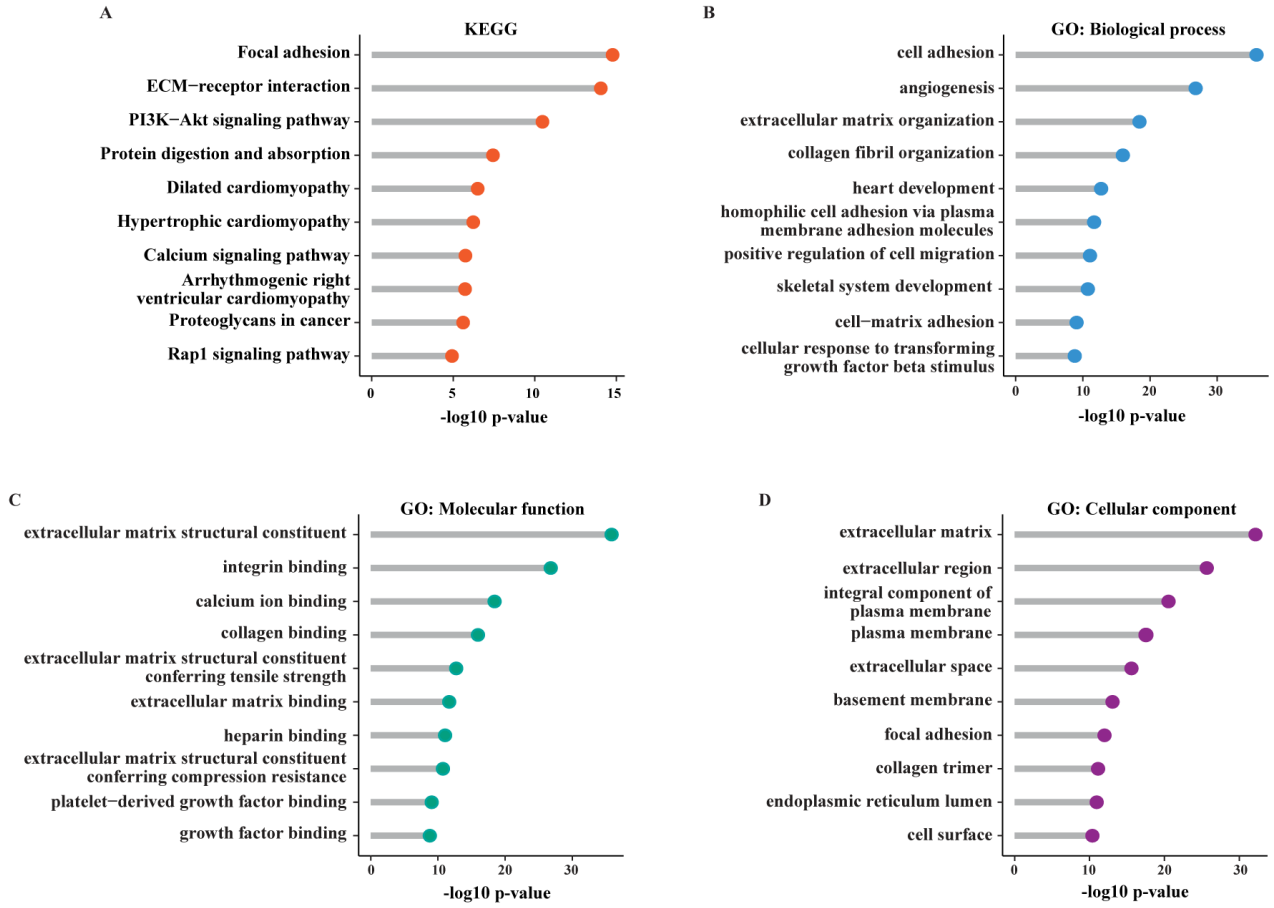

Fig. 3.3.8 EphA3 expression correlates with pro-migratory and invasive genes. KEGG pathway (A) and gene ontology (GO) (B-D) analyses depicting the association of EphA3 expression with pro-metastatic pathways and GO terms in ER-positive BC samples of TCGA. The x-axes and the y-axes indicate respectively the -log10 p-value and the different KEGG pathways and GO terms. Lum A, Luminal A; Lum B, Luminal B; ns, not significant; (**) indicates $p < 0.01$; (***) indicates $p < 0.001$ and (****) indicates $p < 0.0001$.

3.4 The RAGE-dependent EphA3 signaling is involved in the invasive behavior of BC cells and CAFs. Within the tumor microenvironment, CAFs are essential to actively contribute to cancer progression by promoting tumor cell invasion and metastasis (67-68). On these bases and considering that Eph signaling plays a crucial role in the promotion of morphological changes in cancer cells toward their invasion, we first ascertained by real-time PCR experiments that CAFs obtained from

BC patients express both EphA3 and its ligand Ephrin B2 (data not shown). Subsequently, we performed the 3D matrigel drops evasion assay to investigate the role exerted by the EphA3-mediated interaction between BC cells and CAFs toward their pro-invasive behavior. Differently to MCF7/RAGE cells, MCF7/wt cells did not display any ability to migrate from the drop of Matrigel (Fig.3.4.1 A-B). Notably, the EphA3 kinase inhibitor AWL-II-38.3 prevented the motility of both MCF7/RAGE cells and CAFs (Fig. 3.4.1 A-B). All together, these findings indicate that the forward EphA3 transduction pathway, which occurs after the physical interaction between RAGE-overexpressing BC cells and CAFs, mediates the motile phenotype of both cell lines.

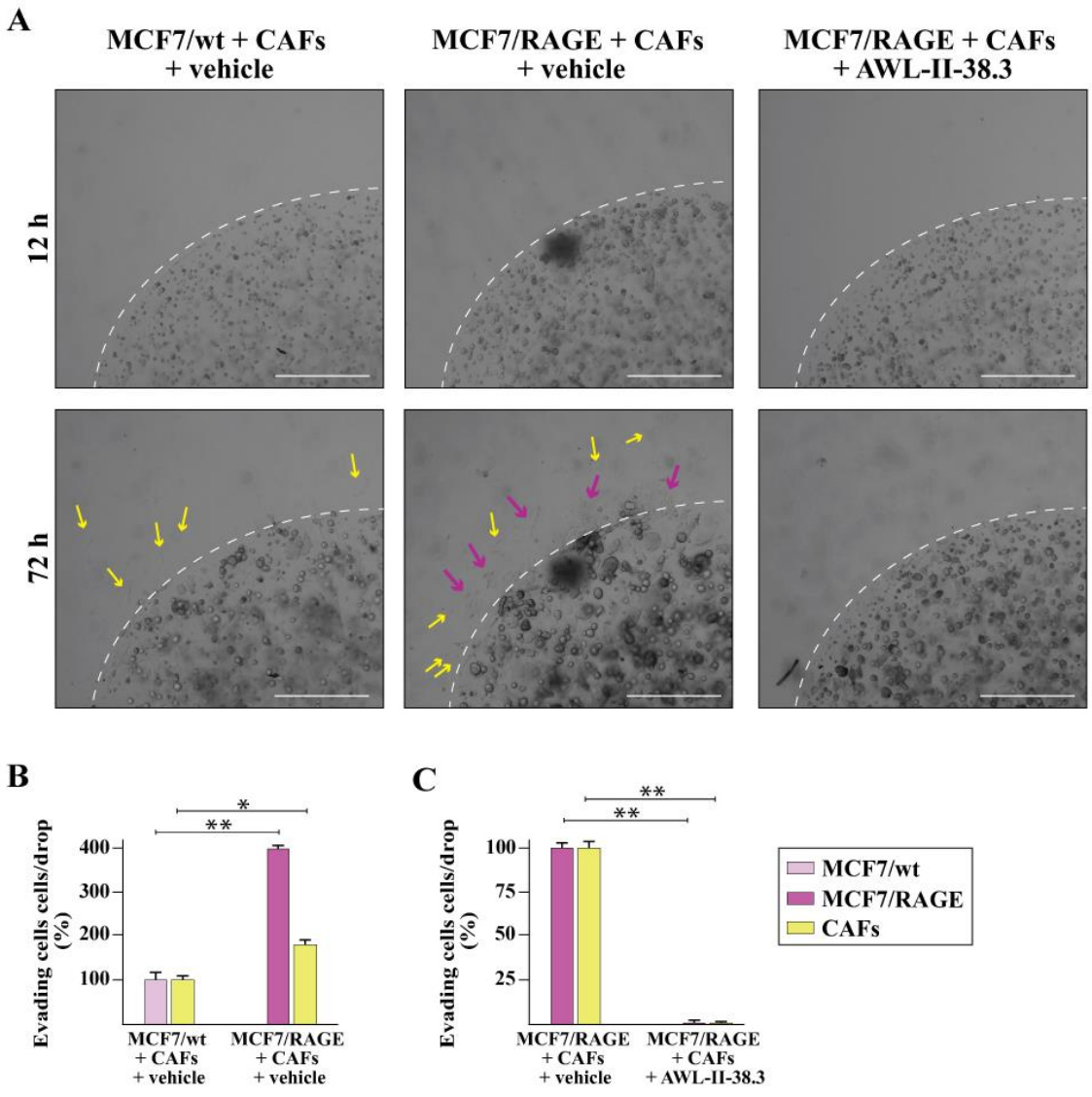

Fig.3.4.1. The evasion of RAGE-overexpressing BC cells and CAFs from Matrigel drops requires the EphA3 transduction pathway. (A) Representative phase contrast images from the Matrigel drops evasion assay from co-cultures of MCF7/wt or MCF7/RAGE cells and CAFs in the presence or absence of 10μM EphA3 inhibitor AWL-II-38.3. (B-C) Percentage of cells around the drop upon 3 days treatment from three independent experiments performed in triplicate. Yellow arrows indicate CAFs. Purple arrows indicate MCF7/RAGE cells. The dotted line indicates the border of drop; scale bar: 650 μm. (*) indicates $p < 0.05$; (**) indicates $p < 0.01$.

4. Discussion

BC is the most common malignancy and the leading cause of cancer-related death among women (69). Obesity and T2DM are known risk factors for the development of BC. In addition, they are both associated with a shorter recurrence time and a greater mortality in women affected by BC (70-75). The chronic metabolic and inflammatory changes associated with obesity and T2DM can create specific condition that promotes the initiation and progression of BC. In this vein, adipokines, hormones and growth factors, hyperglycemia and dyslipidemia may link both obesity and T2DM to BC, thus sustaining the release of pro-tumorigenic inflammatory mediators (70,75,76). As RAGE is over-expressed and hyper-activated in both obese and diabetic individuals (77–79), it has been indicated as a molecular linker of obesity and T2DM to breast tumorigenesis (37,80). In particular, high levels of main RAGE ligands, such as AGEs, HMGB1 and S100 proteins, in both diabetic and obese patients can l trigger the RAGE-mediated activation of pro-inflammatory signaling pathways toward the progression of several human cancers including BC (77,81–91). Further corroborating these findings, increased expression levels of RAGE in BC patients have been associated with adverse clinical features, including advanced-stage disease, tumor size and worse survival outcome (60, 92-93). Despite the numerous evidence suggesting RAGE levels as a prognostic indicator for BC patients, the molecular and functional role of this receptor in ER-positive BC remains to be better appreciated. In this study, we aimed to provide the whole RAGE-dependent transcriptomic changes in ER-positive BC that were manipulated to stably overexpress RAGE. In accordance with RNA-seq data and subsequent GO enrichment analyses indicating that the expression of genes implicated in cell adhesion and chemotaxis processes significantly increases in RAGE-overexpressing respect to wild type BC cells, we demonstrated that RAGE may lead to a motile morphology and behavior of BC cells both *in vitro* and in zebrafish xenograft models.

Eph receptor represent the largest family of the tyrosine kinase receptors. They are able to mediate physical cell–cell communication, and therefore intracellular signaling pathways, by interacting with membrane-associated ligands, the so called ephrins, which are located on neighboring cells.

Eph receptor–ephrin complexes can emanate two different bidirectional events that play a role in both receptor- and ligand-expressing cells toward the control of cell survival, proliferation, differentiation, cell-cell and cell-ECM adhesion, motility and invasion (94, 95). In particular, ligand binding to Eph receptors triggers the "forward" signaling that involves the activation of the kinase domain and is propagated into the Eph receptor-expressing cells (96). Conversely, reverse signals are propagated into the ligand-expressing cells and require the activation of Src family kinases (97). In line with previous findings reporting that EphA3 is highly expressed in lymph node metastases and promotes invasive features in diverse tumors, including BC (98, 99-101), we have ascertained that RAGE-overexpressing BC cells exhibit increased levels of EphA3 and higher invasive skills compared to wild type cells both *in vitro* and *in vivo*. In particular, our data show that the EphA3 forward signaling is involved in the motile behavior of RAGE-overexpressing BC cells, as demonstrated by the use of a EphA3 kinase inhibitor. In the framework of these findings, we have demonstrated that high EphA3 levels may predict a poor prognosis in ER-positive BC patients. In accordance with the above-described experimental data bioinformatics analyses revealed that BC patients showing high EphA3 levels exhibit a specific gene signature that reflects migratory and invasive effects. Altogether, these findings propose that high RAGE levels may induce important transcriptional events that support BC cell motility.

In order to recognize whether the EphA3 transduction pathway may have also a role in the crosstalk between tumor cells and main components of the BC microenvironment, like CAFs, we performed 3D co-culture motility assays that allowed to determine a bidirectional activation of EphA3 signaling toward invasive properties in both BC cells and CAFs isolated from BC biopsies. In conclusion, our study provides novel insights into the mechanisms through which RAGE may prompt migratory and

invasive features in ER-positive BC cells. Worthy, EphA3 was ascertained as a novel RAGE target gene responsible for the stimulatory effects mediated by this receptor in both BC cells and CAFs, where EphA3 signaling may act as a physical linker (Fig. 4.1).

Overall, these data suggest that RAGE overexpression, which may frequently occur in diabetic and obese women, may exert a stimulatory role in BC progression. Hence, the transcriptional and biological routes triggered by RAGE in ER-positive BC cells as well as the EphA3-mediated cooperation between BC cells and CAFs should be taken into account for the assessment of novel therapeutic approaches halting BC progression, particularly in patients also affected by diabetes or obesity.

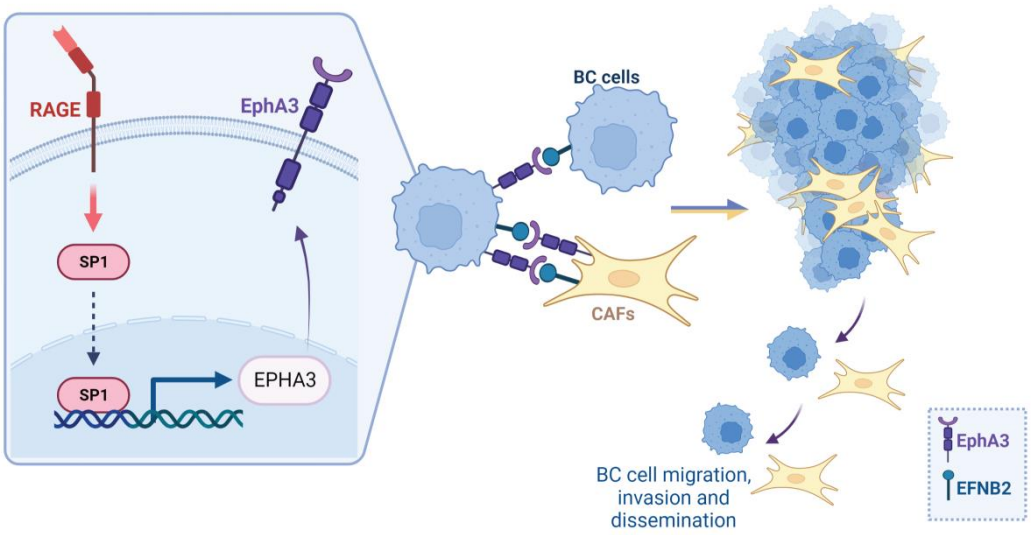

Fig.4.1. Graphical representation of the molecular routes engaged in the stimulatory action elicited by RAGE within the BC microenvironment. Created with BioRender

References

1.Siegel R, Miller K, Jemal A. Cancer statistics, 2017. CA CANCER J. CLIN. 2017. 67: 7–30.

2. Carlson RW, Allred DC, Anderson BO, Burstein HJ, Carter WB, Edge SB, et al. BC. Clinical practice guidelines in oncology. J Natl Compr Canc Netw. 2009. 7:122-92.

3. Britt KL, Cuzick J, Phillips KA. Key steps for effective BC prevention. Nat Rev Cancer. 2020;20(8):417-436.

4. Pandey DP, Lappano R, Albanito L, Madeo A, Maggiolini M, Picard D. Estrogenic GPR30 signalling induces proliferation and migration of BC cells through CTGF. EMBO J. 2009. 28: 523–532.

5.Antoniou A, Pharoah PD, Narod S, Risch HA, Eyfjord JE, Hopper JL, et al. Average risks of breast and ovarian cancer associated with BRCA1 or BRCA2 mutations detected in case Series unselected for family history: a combined analysis of 22 studies. Am J Hum Genet. 2003. 72:1117-30.

6. Bernstein L. Epidemiology of endocrine-related risk factors for BC.J Mammary Gland Biol Neoplasia. 2002. 7:3-15.

7. Kushi LH, Sellers TA, Potter JD, Nelson CL, Munger RG, Kaye SA, Folsom AR. Dietary fat and postmenopausal BC. J Natl Cancer Inst. 1992;84(14):1092-9.

8. Lubin F, Wax Y, Modan B. Role of fat, animal protein, and dietary fiber in BC etiology: a case-control study. J Natl Cancer Inst. 1986;77(3):605-12.

9. van den Brandt PA, van't Veer P, Goldbohm RA, Dorant E, Volovics A, Hermus RJ,

Sturmans F. A prospective cohort study on dietary fat and the risk of postmenopausal breast cancer. Cancer Res. 1993;53(1):75-82.

10. Byrne C, Rockett H, Holmes MD. Dietary fat, fat subtypes, and BC risk: lack of an association among postmenopausal women with no history of benign breast disease. Cancer Epidemiol Biomarkers Prev. 2002;11(3):261-5.

11. Baron JA, Newcomb T, Longnecker G, Mittendorf B, Storer KM, Clapp PN, Bogdan T, Yuen F. Cigarette Smoking and BC. Cancer Epidemiology Biomarkers and Prevention. 1996;5:399-403.

12. Marcus PM, Newman B, Millikan RG, Moorman PG, Baird DD, Qaqish B. The association of adolescent cigarette smoking, alcoholic beverage consumption, environmental tobacco smoke, and ionizing radiation with subsequent BC risk (United States). Cancer Causes and Control. 2000;11:271-278.

13. Egan KM, Stampfer MJ, Hunter D, Hankinson S, Rosner BA, Holmes S, Willet J, Colditz A. Active and passive smoking in BC: prospective results from the Nurses' Health Study. Epidemiology. 2002;13:138-145.

14. Biglia N, Defabiani E, Ponzone R, Mariani L, Marenco D, Sismondi P. Management of risk of breast carcinoma in postmenopausalwomen. Endocrine-Related Cancer. 2004.11:69-83

15. Hazard HW, Hansen NM. Sentinel lymphadenectomy in breast cancer. Cancer Treat Res. 2008;141:11-36. doi: 10.1007/978-0-387-73161-2_2.

16. Carlson RW, Allred DC, Anderson BO, Burstein HJ, Carter WB, Edge SB, Erban JK, Farrar WB, Goldstein LJ, Gradishar WJ, Hayes DF, Hudis CA, Jahanzeb M, Kiel K, Ljung BM, Marcom PK,

Mayer IA, McCormick B, Nabell LM, Pierce LJ, Reed EC, Smith ML, Somlo G, Theriault RL, Topham NS, Ward JH, Winer EP, Wolff AC; NCCN Breast Cancer Clinical Practice Guidelines Panel. Breast cancer. Clinical practice guidelines in oncology. J Natl Compr Canc Netw. 2009 Feb;7(2):122-92. doi: 10.6004/jnccn.2009.0012.

17. Sorlie T, Perou CM, Tibshirani R, Aas T, Geisler S, Johnsen H, Hastie T, Eisen MB, van de Rijn M, Jeffrey SS, Thorsen T, Quist H, Matese JC, Brown PO, Botstein D, Lonning PE, Borresen-Dale AL. Gene expression patterns of breast carcinomas distinguish tumor subclasses with clinical implications. Proc Natl Acad Sci U S A. 2001;98(19):10869-74.

18. Bianchini G, Balko JM, Mayer IA, Sanders ME, Gianni L. Triple-negative BC: challenges and opportunities of a heterogeneous disease. Nat Rev Clin Oncol. 2016;13(11):674-690.

19. Ma XJ, Dahiya S, Richardson E, Erlander M, Sgroi DC. Gene expression profiling of the tumor microenvironment during BC progression. BC Res. 2009. 11:R7.

20. Mittal S, Brown NJ, Holen I. The breast tumor microenvironment: role in cancer development, progression and response to therapy. Expert Rev Mol Diagn. 2018 Mar;18(3):227-243. doi: 10.1080/14737159.2018.1439382. Epub 2018 Feb 15. PMID: 29424261.

21. Orimo A, Gupta PB, Sgroi DC, Arenzana-Seisdedos F, Delaunay T, Naeem R, et al. Stromal fibroblasts present in invasive human breast carcinomas promote tumor growth and angiogenesis through elevated SDF-1/CXCL12 secretion. Cell. 2005. 121:335–348.

22. Polyak K, Hahn WC. Roots and stems: stem cells in cancer. Nat Med. 2006. 12:296–300.

23. Lappano R, Rigiracciolo DC, Belfiore A, Maggiolini M, De Francesco EM. Cancer

associated fibroblasts: role in BC and potential as therapeutic targets. Expert Opin Ther Targets. 2020;24(6):559-572.

24. Hinz B, Phan SH, Thannickal VJ, Prunotto M, Desmoulière A, Varga J, et al. Recent developments in myofibroblast biology: paradigms for connective tissue remodeling. Am J Pathol. 2012. 180:1340–55.

25. Mitra AK, Zillhardt M, Hua Y, Tiwari P, Murmann AE, Peter ME, et al. MicroRNAs reprogram normal fibroblasts into cancer-associated fibroblasts in ovarian cancer. Cancer Discov. 2012. 2:1100–8.

26. Sabbah M, Emami S, Redeuilh G, Julien S, Prévost G, Zimber A, et al. Molecular signature and therapeutic perspective of the epithelial-to-mesenchymal transitions in epithelial cancers. Drug Resist Updat. 2008. 11:123–51.

27. Takebe N, Ivy P, Timmer W, Khan N, Schulz T, Harris PJ. Review of cancer—associated fibroblasts and therapies that interfere with their activity. Tum Microenvir and Ther. 2013. 1:19–36.

28. Togo S, Polanska UM, Horimoto Y, Orimo A. Carcinoma-associated fibroblasts are a promising therapeutic target. Cancers. 2013. 5:149–69.

29. Torre LA, Bray F, Siegel RL, Ferlay J, Lortet-Tieulent J, Jemal A. Global cancer statistics, 2012. CA Cancer J Clin. 2015;65(2):87-108ca. PMID: 11578972.

30. Chen X, Song E. Turning foes to friends: targeting cancer-associated fibroblasts. Nat Rev Drug Discov. 2019 Feb;18(2):99-115. doi: 10.1038/s41573-018-0004-1.

31. Buckley ST, Ehrhardt C. The receptor for advanced glycation end products (RAGE) and the lung. J Biomed Biotechnol. 2010;2010:917108. doi: 10.1155/2010/917108. Epub 2010 Jan 19.

32. Lee EJ, Park JH. Receptor for Advanced Glycation Endproducts (RAGE), Its Ligands, and Soluble RAGE: Potential Biomarkers for Diagnosis and Therapeutic Targets for Human Renal Diseases. Genomics Inform. 2013 Dec;11(4):224-9. doi: 10.5808/GI.2013.11.4.224.

33. Rojas A, González I, Morales E, Pérez-Castro R, Romero J, Figueroa H. Diabetes and cancer: Looking at the multiligand/RAGE axis. World J Diabetes. 2011 Jul 15;2(7):108-13. doi: 10.4239/wjd.v2.i7.108. PMID: 21860695; PMCID: PMC3158864.

34. Logsdon CD, Fuentes MK, Huang EH, Arumugam T. RAGE and RAGE ligands in cancer. Curr Mol Med. 2007;7:777–89.

35. Zhang Z, Wang M, Zhou L, Feng X, Cheng J, Yu Y, et al. Increased HMGB1 and cleaved caspase-3 stimulate the proliferation of tumor cells and are correlated with the poor prognosis in colorectal cancer. J Exp Clin Cancer Res. 2015;34:51.

36. Kwak T, Drews-Elger K, Ergonul A, Miller PC, Braley A, Hwang GH, et al. Targeting of RAGE-ligand signaling impairs BC cell invasion and metastasis. Oncogene. 2017;36:1559–72.

37. Mishra S, Charan M, Shukla RK, Agarwal P, Misri S, Verma AK, et al. cPLA2 blockade attenuates S100A7-mediated breast tumorigenicity by inhibiting the immunosuppressive tumor microenvironment. J Exp Clin Cancer Res. 2022;41:54.

38. Palanissami G, Paul SFD. RAGE and Its Ligands: Molecular Interplay Between Glycation, Inflammation, and Hallmarks of Cancer-a Review. Horm Cancer. 2018;9:295–325.

39. Muoio MG, Talia M, Lappano R, Sims AH, Vella V, Cirillo F, et al. Activation of the S100A7/RAGE Pathway by IGF-1 Contributes to Angiogenesis in BC. Cancers [Internet]. 2021;13. Available from: http://dx.doi.org/10.3390/cancers13040621

40. Himanen JP, Nikolov DB. Eph receptors and ephrins. Int J Biochem Cell Biol. 2003 Feb;35(2):130-4. doi: 10.1016/s1357-2725(02)00096-1. PMID: 12479863.

41. Boyd AW, Lackmann M. Signals from Eph and ephrin proteins: a developmental tool kit. Sci STKE. 2001 Dec 11;2001(112):re20. doi: 10.1126/stke.2001.112.re20. PMID: 11741094.

42. Surawska H, Ma PC, Salgia R. The role of ephrins and Eph receptors in cancer. Cytokine Growth Factor Rev. 2004 Dec;15(6):419-33. doi: 10.1016/j.cytogfr.2004.09.002. PMID: 15561600.

43. Singh A, Winterbottom E, Daar IO. Eph/ephrin signaling in cell-cell and cell-substrate adhesion. Front Biosci (Landmark Ed). 2012 Jan 1;17(2):473-97. Doi: 10.2741/3939.

44. Easty DJ, Guthrie BA, Maung K, Farr CJ, Lindberg RA, Toso RJ, Herlyn M, Bennett DC. Protein B61 as a new growth factor: expression of B61 and up-regulation of its receptor epithelial cell kinase during melanoma progression. Cancer Res. 1995 Jun 15;55(12):2528-32. PMID: 7780963.

45. Berclaz G, Andres AC, Albrecht D, Dreher E, Ziemiecki A, Gusterson BA, Crompton MR. Expression of the receptor protein tyrosine kinase myk-1/htk in normal and malignant mammary epithelium. Biochem Biophys Res Commun. 1996 Sep 24;226(3):869-75. doi: 10.1006/bbrc.1996.1442. PMID: 8831703

46. Astin JW, Batson J, Kadir S, Charlet J, Persad RA, Gillatt D, Oxley JD, Nobes CD. Competition amongst Eph receptors regulates contact inhibition of locomotion and invasiveness in prostate cancer cells. Nat Cell Biol. 2010 Dec;12(12):1194-204. doi: 10.1038/ncb2122. Epub 2010 Nov 14. PMID: 21076414.

47. Huttunen HJ, Fages C, Rauvala H. Receptor for advanced glycation end products (RAGE)-mediated neurite outgrowth and activation of NF-kappaB require the cytoplasmic domain of the receptor but different downstream signaling pathways. J Biol Chem. 1999;274:19919–24.

48. Lappano R, Talia M, Cirillo F, Rigiracciolo DC, Scordamaglia D, Guzzi R, et al. The IL1β-IL1R signaling is involved in the stimulatory effects triggered by hypoxia in BC cells and cancer-associated fibroblasts (CAFs). J Exp Clin Cancer Res. 2020;39:153.

49. Chen S, Zhou Y, Chen Y, Gu J. fastp: an ultra-fast all-in-one FASTQ preprocessor. Bioinformatics. 2018;34:i884–90.

50. Dobin A, Davis CA, Schlesinger F, Drenkow J, Zaleski C, Jha S, et al. STAR: ultrafast universal RNA-seq aligner. Bioinformatics. 2013;29:15–21.

51. Li B, Dewey CN. RSEM: accurate transcript quantification from RNA-Seq data with or without a reference genome. BMC Bioinformatics. 2011;12:323.

52. McCarthy DJ, Chen Y, Smyth GK. Differential expression analysis of multifactor RNA-Seq experiments with respect to biological variation. Nucleic Acids Res. 2012;40:4288–97.

53. Durinck S, Spellman PT, Birney E, Huber W. Mapping identifiers for the integration of genomic datasets with the R/Bioconductor package biomaRt. Nat Protoc. 2009;4:1184–91.

54. Pearce DA, Nirmal AJ, Freeman TC, Sims AH. Continuous Biomarker Assessment by Exhaustive Survival Analysis [Internet]. bioRxiv. 2018 [cited 2023 Mar 8]. p. 208660. Available from: https://www.biorxiv.org/content/10.1101/208660v2

55. Alexa A, Rahnenfuhrer J. topGO: Enrichment Analysis for Gene Ontology (2.46. 0)[Computer software]. Bioconductor version: Release (3.14). 2022;

56. Cirillo F, Lappano R, Bruno L, Rizzuti B, Grande F, Guzzi R, et al. AHR and GPER mediate the stimulatory effects induced by 3-methylcholanthrene in BC cells and cancer-associated fibroblasts (CAFs). J Exp Clin Cancer Res. 2019;38:335.

57. Scordamaglia D, Cirillo F, Talia M, Santolla MF, Rigiracciolo DC, Muglia L, et al. Metformin counteracts stimulatory effects induced by insulin in primary BC cells. J Transl Med. 2022;20:263.

58. Aslan M, Hsu E-C, Liu S, Stoyanova T. Quantifying the invasion and migration ability of cancer cells with a 3D Matrigel drop invasion assay. Biol Methods Protoc. 2021;6:bpab014.

59. Kimmel CB, Ballard WW, Kimmel SR, Ullmann B, Schilling TF. Stages of embryonic development of the zebrafish. Dev Dyn. 1995;203:253–310.

60. Rigiracciolo DC, Nohata N, Lappano R, Cirillo F, Talia M, Adame-Garcia SR, et al. Focal Adhesion Kinase (FAK)-Hippo/YAP transduction signaling mediates the stimulatory effects exerted by S100A8/A9-RAGE system in triple-negative BC (TNBC). J Exp Clin Cancer Res. 2022;41:193.

61. Jacquemet G, Hamidi H, Ivaska J. Filopodia in cell adhesion, 3D migration and cancer cell invasion. Curr Opin Cell Biol. 2015;36:23–31.

62. Jacquemet G, Paatero I, Carisey AF, Padzik A, Orange JS, Hamidi H, et al. FiloQuant reveals increased filopodia density during BC progression. J Cell Biol. 2017;216:3387–403.

63. Teng Y, Mei Y, Hawthorn L, Cowell JK. WASF3 regulates miR-200 inactivation by ZEB1 through suppression of KISS1 leading to increased invasiveness in BC cells. Oncogene. 2014;33:203–11.

64. Razak NA, Abu N, Ho WY, Zamberi NR, Tan SW, Alitheen NB, et al. Cytotoxicity of eupatorin in MCF-7 and MDA-MB-231 human BC cells via cell cycle arrest, anti-angiogenesis and induction of apoptosis. Sci Rep. 2019;9:1514.

65. Pasquale EB. Eph receptors and ephrins in cancer: bidirectional signalling and beyond. Nat Rev Cancer. 2010;10:165–80.

66. Diao X, Chen X, Pi Y, Zhang Y, Wang F, Liu P, et al. Androgen receptor induces EPHA3 expression by interacting with transcription factor SP1. Oncol Rep. 2018;40:1174–84.

67. Hanahan D, Coussens LM. Accessories to the crime: functions of cells recruited to the tumor microenvironment. Cancer Cell. 2012;21:309–22.

68. Sahai E, Astsaturov I, Cukierman E, DeNardo DG, Egeblad M, Evans RM, et al. A framework for advancing our understanding of cancer-associated fibroblasts. Nat Rev Cancer. 2020;20:174–86.

69. Sung H, Ferlay J, Siegel RL, Laversanne M, Soerjomataram I, Jemal A, et al. Global Cancer Statistics 2020: GLOBOCAN Estimates of Incidence and Mortality Worldwide for 36 Cancers in 185 Countries. CA Cancer J Clin. 2021;71:209–49.

70. Kang C, LeRoith D, Gallagher EJ. Diabetes, Obesity, and BC. Endocrinology. 2018;159:3801–12.

71. Protani M, Coory M, Martin JH. Effect of obesity on survival of women with BC: systematic review and meta-analysis. BC Res Treat. 2010;123:627–35.

72. Larsson SC, Mantzoros CS, Wolk A. Diabetes mellitus and risk of BC: a meta-analysis. Int J Cancer. 2007;121:856–62.

73. Neuhouser ML, Aragaki AK, Prentice RL, Manson JE, Chlebowski R, Carty CL, et al. Overweight, Obesity, and Postmenopausal Invasive BC Risk: A Secondary Analysis of the Women's Health Initiative Randomized Clinical Trials. JAMA Oncol. 2015;1:611–21.

74. Renehan AG, Tyson M, Egger M, Heller RF, Zwahlen M. Body-mass index and incidence of cancer: a systematic review and meta-analysis of prospective observational studies. Lancet. 2008;371:569–78.

75. Picon-Ruiz M, Morata-Tarifa C, Valle-Goffin JJ, Friedman ER, Slingerland JM. Obesity and adverse BC risk and outcome: Mechanistic insights and strategies for intervention. CA Cancer J Clin. 2017;67:378–97.

76. Zhou X, Zhang J, Lv W, Zhao C, Xia Y, Wu Y, et al. The pleiotropic roles of adipocyte secretome in remodeling BC. J Exp Clin Cancer Res. 2022;41:203.

77. Feng Z, Zhu L, Wu J. RAGE signalling in obesity and diabetes: focus on the adipose tissue macrophage. Adipocyte. 2020;9:563–6.

78. Uribarri J, Cai W, Ramdas M, Goodman S, Pyzik R, Chen X, et al. Restriction of advanced glycation end products improves insulin resistance in human type 2 diabetes: potential role of AGER1 and SIRT1. Diabetes Care. 2011;34:1610–6.

79. Feng Z, Du Z, Shu X, Zhu L, Wu J, Gao Q, et al. Role of RAGE in obesity-induced adipose tissue inflammation and insulin resistance. Cell Death Discov. 2021;7:305.

80. Vella V, Lappano R, Bonavita E, Maggiolini M, Clarke RB, Belfiore A, et al. Insulin/IGF axis and the Receptor for Advanced Glycation End Products: role in meta-inflammation and potential in cancer therapy. Endocr Rev [Internet]. 2023; Available from: http://dx.doi.org/10.1210/endrev/bnad005;

81. Rojas A, González I, Morales E, Pérez-Castro R, Romero J, Figueroa H. Diabetes and cancer: Looking at the multiligand/RAGE axis. World J Diabetes. 2011;2:108–13.

82. Tan KCB, Chow W-S, Ai VHG, Metz C, Bucala R, Lam KSL. Advanced glycation end products and endothelial dysfunction in type 2 diabetes. Diabetes Care. 2002;25:1055–9.

83. Chen M-C, Chen K-C, Chang G-C, Lin H, Wu C-C, Kao W-H, et al. RAGE acts as an oncogenic role and promotes the metastasis of human lung cancer. Cell Death Dis. 2020;11:265.

84. Pan S, Guan Y, Ma Y, Cui Q, Tang Z, Li J, et al. Advanced glycation end products correlate with BC metastasis by activating RAGE/TLR4 signaling. BMJ Open Diabetes Res Care [Internet]. 2022;10. Available from: http://dx.doi.org/10.1136/bmjdrc-2021-002697

85. Omofuma OO, Peterson LL, Turner DP, Merchant AT, Zhang J, Thomson CA, et al. Dietary Advanced Glycation End-Products and Mortality after BC in the Women's Health Initiative. Cancer Epidemiol Biomarkers Prev. 2021;30:2217–26.

86. Sharaf H, Matou-Nasri S, Wang Q, Rabhan Z, Al-Eidi H, Al Abdulrahman A, et al. Advanced glycation endproducts increase proliferation, migration and invasion of the BC cell line MDA-MB-231. Biochim Biophys Acta. 2015;1852:429–41.

87. Santolla MF, Talia M, Cirillo F, Scordamaglia D, De Rosis S, Spinelli A, et al. The AGEs/RAGE Transduction Signaling Prompts IL-8/CXCR1/2-Mediated Interaction between Cancer-Associated Fibroblasts (CAFs) and BC Cells. Cells [Internet]. 2022;11. Available from: http://dx.doi.org/10.3390/cells11152402

88. Nasser MW, Wani NA, Ahirwar DK, Powell CA, Ravi J, Elbaz M, et al. RAGE mediates S100A7-induced BC growth and metastasis by modulating the tumor microenvironment. Cancer Res. 2015;75:974–85.

89. Muthyalaiah YS, Jonnalagadda B, John CM, Arockiasamy S. Impact of Advanced Glycation End products (AGEs) and its receptor (RAGE) on cancer metabolic signaling pathways and its progression. Glycoconj J. 2021;38:717–34.

90. Leung SS, Forbes JM, Borg DJ. Receptor for Advanced Glycation End Products (RAGE) in Type 1 Diabetes Pathogenesis. Curr Diab Rep. 2016;16:100.

91. Chen Y, Cai L, Guo X, Li Z, Liao X, Zhang X, et al. HMGB1-activated fibroblasts promote BC cells metastasis via RAGE/aerobic glycolysis. Neoplasma. 2021;68:71–8.

92. Nankali M, Karimi J, Goodarzi MT, Saidijam M, Khodadadi I, Razavi ANE, et al. Increased Expression of the Receptor for Advanced Glycation End-Products (RAGE) Is Associated with Advanced BC Stage. Oncol Res Treat. 2016;39:622–8.

93. Hsieh H-L, Schäfer BW, Sasaki N, Heizmann CW. Expression analysis of S100 proteins and RAGE in human tumors using tissue microarrays. Biochem Biophys Res Commun. 2003;307:375–81.

94. Wang B. Cancer cells exploit the Eph-ephrin system to promote invasion and metastasis: tales of unwitting partners. Sci Signal. 2011;4:e28.

95. Kandouz M. The Eph/Ephrin family in cancer metastasis: communication at the service of invasion. Cancer Metastasis Rev. 2012;31:353–73

96. Pasquale EB. Eph receptors and ephrins in cancer: bidirectional signalling and beyond. Nat Rev Cancer. 2010 Mar;10(3):165-80. doi: 10.1038/nrc2806.

97. Holen HL, Shadidi M, Narvhus K, Kjøsnes O, Tierens A, Aasheim HC. Signaling through ephrin-A ligand leads to activation of Src-family kinases, Akt phosphorylation, and inhibition of antigen receptor-induced apoptosis. J Leukoc Biol. 2008 Oct;84(4):1183-91. doi: 10.1189/jlb.1207829.

98. Nasri B, Inokuchi M, Ishikawa T, Uetake H, Takagi Y, Otsuki S, et al. High expression of EphA3 (erythropoietin-producing hepatocellular A3) in gastric cancer is associated with metastasis and poor survival. BMC Clin Pathol. 2017;17:8.

99. Lu C-Y, Yang Z-X, Zhou L, Huang Z-Z, Zhang H-T, Li J, et al. High levels of EphA3 expression are associated with high invasive capacity and poor overall survival in hepatocellular carcinoma. Oncol Rep. 2013;30:2179–86.

100. Xi H-Q, Wu X-S, Wei B, Chen L. Aberrant expression of EphA3 in gastric carcinoma: correlation with tumor angiogenesis and survival. J Gastroenterol. 2012;47:785–94.

101. Vail ME, Murone C, Tan A, Hii L, Abebe D, Janes PW, et al. Targeting EphA3 inhibits cancer growth by disrupting the tumor stromal microenvironment. Cancer Res. 2014;74:4470–81.

Pubblications

1. Cirillo F, Pellegrino M, Talia M, Perrotta ID, Rigiracciolo DC, Spinelli A, Scordamaglia D, Muglia L, Guzzi R, Miglietta AM, De Francesco EM, Belfiore A, Maggiolini M, Lappano R. Estrogen receptor variant ERα46 and insulin receptor drive in primary breast cancer cells growth effects and interleukin 11 induction prompting the motility of cancer-associated fibroblasts. Clin Transl Med. 2021 Nov;11(11):e516. doi: 10.1002/ctm2.516.

2. Santolla MF, Talia M, Cirillo F, Scordamaglia D, De Rosis S, Spinelli A, Miglietta AM, Nardo B, Filippelli G, De Francesco EM, Belfiore A, Lappano R, Maggiolini M. The AGEs/RAGE Transduction Signaling Prompts IL-8/CXCR1/2-Mediated Interaction between Cancer-Associated Fibroblasts (CAFs) and Breast Cancer Cells. Cells. 2022 Aug 4;11(15):2402. doi: 10.3390/cells11152402.

3. Cirillo F, Talia M, Santolla MF, Pellegrino M, Scordamaglia D, Spinelli A, De Rosis S, Giordano F, Muglia L, Zicarelli A, Di Dio M, Rigiracciolo DC, Miglietta AM, Filippelli G, De Francesco EM, Belfiore A, Lappano R, Maggiolini M. GPER deletion triggers inhibitory effects in triple negative breast cancer (TNBC) cells through the JNK/c-Jun/p53/Noxa transduction pathway. Cell Death Discov. 2023 Sep 26;9(1):353. doi: 10.1038/s41420-023-01654-0.

4. Talia M*, Cirillo F*, Spinelli A*, Zicarelli A, Scordamaglia D, Muglia L, De Rosis S, Rigiracciolo DC, Filippelli G, Perrotta ID, Davoli M, De Rosa R, Macirella R, Brunelli E, Miglietta AM, Nardo B, Tosoni D, Pece S, De Francesco EM, Belfiore A, Maggiolini M, Lappano R. The Ephrin tyrosine kinase a3 (EphA3) is a novel mediator of RAGE-prompted motility of breast cancer cells. J Exp Clin Cancer Res. 2023 Jul 12;42(1):164. doi: 10.1186/s13046-023-02747-5. *: Co-first Authors.